Am J Cancer Res 2022;12(7):2989-3013
www.ajcr.us /ISSN:2156-6976/ajcr0142213

Original Article

RNA methylation regulators contribute to poor prognosis of hepatocellular carcinoma associated with the suppression of bile acid metabolism: a multi-omics analysis

Tao Zhang[1*], Jian Gu[1*], Xinyi Wang[3], Jiajia Luo[1], Jing Yan[1], Kailin Cai[3], Huili Li[3], Yingli Nie[2], Xiangdong Chen[1], Jiliang Wang[3]

[1]Department of Anesthesiology, Union Hospital, Tongji Medical College, Huazhong University of Science and Technology, Wuhan 430022, China; [2]Department of Dermatology, Wuhan Children's Hospital (Wuhan Maternal and Child Healthcare Hospital), Tongji Medical College, Huazhong University of Science and Technology, Wuhan 430014, China; [3]Department of Gastrointestinal Surgery, Union Hospital, Tongji Medical College, Huazhong University of Science and Technology, Wuhan 430022, China. [*]Equal contributors.

Received February 7, 2022; Accepted June 9, 2022; Epub July 15, 2022; Published July 30, 2022

Abstract: RNA methylation has been known to promote the initiation and progression of many types of cancer, including hepatocellular carcinoma (HCC). To fully understand the importance of this post-transcriptional modification in HCC, a thorough investigation that combines different patterns of RNA methylation is urgently needed. In this study, we investigated the regulators of the three most common types of RNA methylation: m6A, N1-methyladenosine (m1A) and 5-methylcytosine (m5C). Based on the genomic and proteomic data, we constructed a classifier consisting of seven RNA methylation regulators. This classifier performed well and robustly predicted the prognosis of HCC patients. By analysis using this classifier, we found that the primary bile acid biosynthesis pathway was mostly downregulated in high-risk HCC patients. Furthermore, we found that the gene expression patterns regulated by several bile acids were similar to those regulated by some well-defined anti-tumor compounds, indicating that bile acid metabolism plays a crucial role in the progression of HCC, and the related metabolites can be used as the potential agents for HCC treatments. Moreover, our study revealed a crosstalk between RNA methylation and bile acid regulators, demonstrating a novel mechanism of the downregulation of bile acid metabolism in HCC and providing new insights into how RNA methylation regulators affect the oncogenesis of HCC.

Keywords: Hepatocellular carcinoma, N6-methyladenosine, N1-methyladenosine, 5-methylcytosine, prognosis, bile acid

Introduction

Hepatocellular carcinoma (HCC) is one of the most prevalent malignancies and is currently the seventh and fifth leading cause of cancer-related deaths in men and women worldwide, respectively [1]. Despite the advancement in early diagnosis, surgical treatment and immunotherapy, the long-term prognosis of HCC is still poor. Therefore, constructing an effective prognostic model to identify high-risk HCC patients with poor prognoses is crucial for the personalized treatment and improved prognosis of HCC patients.

Recently, increasing evidence indicates that RNA modification is an important mechanism for the epigenetic regulation of gene expression and plays a key role in a variety of physiological and pathological processes. There are currently more than 170 distinct RNA modifications. Of these, RNA methylation, including m6A, N1-methyladenosine (m1A), 5-methylcytosine (m5C), and 2'-O-methylation (Nm), represents more than half of the RNA modifications [2]. RNA methylation plays a critical role in regulating gene expression via regulating transcription and translation. This post-transcriptional modification is controlled by regulators known as

"writers" (methyltransferases), "readers" and "erasers" (demethylase). RNA methylation has been found to be associated with the occurrence and progression of various cancers, and some of the regulators have been identified as cancer biomarkers [3-5]. However, most studies focus only on m6A and several other common types of RNA methylation [6].

m6A, which refers to the addition of a methyl group at the N6 position of adenosine, is the most abundant RNA modification in eukaryotic cells. m6A modification is mediated by three classes of proteins: m6A-modified site recognizing proteins, methyl group transferring proteins, and methyl group removing proteins, respectively. The m6A methyl group transfer process is mediated by methyltransferases, including METTL3, METTL14, RBM15, RBM15B, WTAP, KIAA1429, CBLL1, VIRMA and ZC3H13, while the methyl group removal process is catalyzed by demethylases, including FTO and ALKBH5. A group of proteins, including YTHDC1/2, YTHDF1/2/3, HNRNPA2B1, HNRNPC, LRPPRC, FMR1 and ELAVL1, can specifically recognize m6A modification sites to initiate the m6A modification process [7]. m6A modification plays crucial roles in the carcinogenesis of many cancer types, including HCC [7]. For example, Chen et al. has reported that methyltransferase METTL3 promotes HCC progression through mediating m6A modification at the 3' end of the mRNA encoding suppressor of cytokine signaling 2 (SOCS2), leading to SOCS2 mRNA degradation through a YTHDF2-dependent manner [8]. In addition, METTL3 also regulates the process of epithelial-mesenchymal transition (EMT), promoting the invasion and metastasis of HCC [9]. Compared with normal liver tissues, demethylase FTO is overexpressed in HCC, which is associated with a poor prognosis. The knockdown of FTO leads to cell cycle arrest and suppresses the proliferation of HCC cells partially through stimulating the demethylation of pyruvate kinase M2 (PKM2) mRNA [10]. Other m6A regulators, such as IGF2BPs [11], YTHDF2 [12] and METTL14 [13], also act as significant oncogenes and participate in the development of HCC.

Another common RNA methylation is m1A, which is formed by attaching a methyl group to the N1 position of adenosine, and is found in mRNA, tRNA, rRNA and mitochondrial transcripts [14]. The regulators of m1A methylation are composed of "writers" (TRMT6, TRMT61A, TRMT61B and TRMT10C), "erasers" (ALKBH1 and ALKBH3), and "readers" (YTHDF1/2/3 and YTHDC1) [15, 16]. The dysregulation of m1A affects a variety of biological processes, including cell proliferation, apoptosis, and self renewal, all of which have been linked to the progression of various malignancies. For example, eraser ALKBH3 promotes colony-stimulating factor 1 (CSF1) mRNA expression through the demethylation of m1A, resulting to the enhanced invasion of ovarian and breast cancer cells [17]. Additionally, ALKBH3 contributes to the progression of urothelial carcinomas by promoting the survival and invasion of tumor cells through Tweak/Fn14-VEGF and NOX-2-ROS signaling [18]. Recently, Shi et al. have found that m1A regulators, such as YTHDF1, TRMT6, TRMT61A and TRMT10C, effectively predict the prognosis of HCC patients and mediate some important biological processes. The PI3K/Akt and MYC signaling pathways have also been implicated in modifying m1A in HCC cells [19].

Another common methylation in mammalian RNA is m5C, which is found in both mRNAs and non-coding RNAs (ncRNAs: lncRNAs, rRNAs, tRNAs, eRNAs, etc.) [20]. The m5C modification involves "writers" (NOP2, NSUN1-7, DNMT1/2, DNMT2, DNMT3A and DNMT3B), "erasers" (TET1/2/3 and ALKBH1), and "readers" (ALYREF and YBX1) [21]. Increasing evidence has demonstrated that m5C modification plays a vital role in regulating important biological and pathological processes, including cancer [21]. NSUN2, TETs and ALKBH1 are frequently overexpressed in various cancers, suggesting a oncogenic role of m5C in tumorigenesis [22-25]. In addition, Chen et al. have reported that NSUN2 and YBX1 stabilize oncogene hepatoma-derived growth factor (HDGF) mRNA by targeting the m5C modification site in its 3' UTR and, therefore, play oncogenic roles in bladder cancer [26].

To thoroughly understand the importance of RNA methylation in HCC, a comprehensive analysis that includes different patterns of RNA methylation is essential. In this study, we established a classifier consisting of 7 RNA methylation regulators for predicting the prognosis of HCC patients. Based on the risk score

calculated by the classifier, our study samples were divided into low- and high-risk group. We found that the primary bile acid biosynthesis pathway was mostly downregulated in the high-risk group. Since bile acid metabolism and related metabolites play vital roles in the initiation and development of HCC, they could serve as potential targets for anti-HCC treatments. Furthermore, our study identified a crosstalk between RNA methylation and bile acid regulators, suggesting a novel mechanism of the downregulation of bile acid metabolism in HCC and providing new insights into how RNA methylation regulators affect the oncogenesis of HCC.

Materials and methods

Data acquisition and data analysis

The workflow of our bioinformatics analyses was shown in Figure S1. HCC cohorts with patient survival data were obtained from several databases, including GEO (Gene Expression Omnibus: GSE14520, GSE10143, GSE76427 and GSE54236), ICGC (International Cancer Genome Consortium), TCGA (The Cancer Genome Atlas), and CPTAC (Clinical Proteomic Tumor Analysis Consortium). In total, three cohorts were selected, including TCGA-Liver Hepatocellular Carcinoma (TCGA-LIHC), ICGC-Liver Cancer-RIKEN-Japan (LIRI-JP), and CPTAC-HCC cohort.

The mRNA expression (raw counts), somatic mutation, and the clinical information of HCC tissues (n=374) and normal liver tissues (n=50) were downloaded from the TCGA database (https://portal.gdc.cancer.gov and https://xenabrowser.net/datapages/). For validation, the RNA-seq and the clinical information of 232 HCC tumor samples were obtained from the ICGC portal (https://dcc.icgc.org/projects/LIRI-JP). Additionally, the proteogenomics data and the clinical information of HCC tissues (n=165) and their corresponding normal tissues (n=165) were downloaded from the CPTAC database (https://cptac-data-portal.georgetown.edu/). We also used the microarray data and the clinical data of other 81 HCC tumor samples from the GEO database (https://www.ncbi.nlm.nih.gov/geo/geo2r/?acc=GSE54236). The RNA-seq data of the ICGC cohort were transformed by using log2 (counts+1). The RNA-seq data of the TCGA and ICGC cohorts and the proteogenomics data of the CPTAC cohort were shown in Table S1.

A metabolomics dataset of HCC serum metabolites, MTBLS17, was downloaded from European Bioinformatics Institute (EMBL-EBI), which contains 158 samples from HCC patients and 368 samples from non-HCC individuals.

Identification of RNA methylation regulators with prognostic value

A univariate Cox regression was conducted for all RNA methylation regulators based on the expression level of each regulator. Genes with $P<0.05$ were identified as prognostic RNA methylation regulators.

Generation of RNA methylation regulators-based classifier

The most significant prognostic RNA methylation regulators were selected by the 10-fold least absolute shrinkage and selection operator (LASSO) Cox regression analysis. LASSO is a penalized regression method that estimates regression coefficients by maximizing the log-likelihood function (or the sum of squared residuals). By the L1-penalty, the LASSO does variable selection and shrinkage, only retaining the most important variables in the final model. In 10-fold cross validation, the samples were divided into 10 subsets (folds); 9 subsets were used to train the model each time, and then the remaining subset was used as the validation set. Finally, the 10 results were combined to determine the final coefficients [27]. The prognostic risk scores were calculated based on a formula as follows: $Risk\ Score = \Sigma(Genes_{Cox\ coefficient} \times Genes_{expression\ levels})$.

We then divided the HCC patients into low- and high-risk group by using the median risk score as the cut-off value. For validation, the risk scores of samples in ICGC were also calculated by the above formula. According to the cut-off value, ICGC samples were divided into high- and low-risk group. Next, the predictive capability of the classifier for the training and validation cohorts was evaluated using the Kaplan-Meier log-rank test, Receiver Operating

Characteristic (ROC) curve analysis, univariate, and multivariate Cox regression analysis.

Identification of differentially expressed genes (DEGs) and functional annotation

The "limma" package of R was used to identify the differentially expressed gene (DEGs) between high- and low-risk group with the cut-off criteria of |log2 fold change (FC)| >1 and adjusted *P*-value <0.05. Functional enrichment analysis of DEGs was performed using Metascape (https://metascape.org/). P<0.005 was considered statistically significant.

Gene Set Enrichment Analysis (GSEA) and Gene Set Variation Analysis (GSVA) were performed to explore the difference in metabolic pathways between high- and low-risk group. The clusterProfiler R package [28] was employed to perform GSEA analysis based on the Kyoto Encyclopedia of Genes and Genomes (KEGG) database. P<0.01 was considered statistically significant. The GSVA analysis was conducted based on c2.cp.kegg.v7.4.symbols.gmt and c5.go.bp.v7.4.symbols.gmt reference gene set files. After that, we used the "ComplexHeatmap" package to display the distinct pathways between the high- and low-risk groups.

Unsupervised clustering of RNA methylation regulators

Consensus clustering is an unsupervised clustering method that provides quantitative and visual stability for estimating the number of unsupervised categories in a dataset [29]. To deduce the RNA methylation status of a sample, we utilized the Consensus ClusterPlus R packages to classify HCC samples into different categories based on the expression of RNA methylation regulators.

Screening of similar functional compounds to bile acids

The Connectivity Map (cMap) touchstone database (https://clue.io/) includes the gene expression signatures derived from 9 cancer cell lines treated with 2429 well-defined compounds. All compounds are assigned a connectivity score (ranging from -100 to 100) based on the similarity of the gene expression changes they induce, when compared to the others. Positive connectivity scores indicate similar gene expression changes, while negative scores indicate opposing patterns. The gene regulation pattern in HepG2, an HCC cell line, induced by bile acids treatment was obtained from cMap. Compounds with connectivity scores of more than 90 when compared to bile acids were defined as highly similar compounds.

The regulation of bile acid metabolism pathway by RNA methylation regulators

To further explore the relationship between RNA methylation regulators and bile acid metabolism, the potential RNA methylation sites in bile acid metabolism related genes were searched from the RMBase v2.0 database (http://rna.sysu.edu.cn/rmbase/). RMBase v2.0 contains about 1397000 RNA modification sites, including m6A, m1A, pseudouridine (Ψ) and m5C, 2'-O-methylations (2'-O-Me), among 13 species [30]. Next, the potential regulatory role of m6A regulators on bile acid metabolism genes was explored by the m6A-2Target database (http://m6a2target.cancer-omics.org/). The m6A2Target database contains the validated and potential interactions between genes and m6A regulators through extracting all published m6A-related articles and collecting high-throughput sequencing data of CHIP-seq, CLIP-seq, RIP-seq, mass spectrometry, MeRIP-seq and RNA-seq [31]. The regulatory network was constructed by Cytoscape software. Finally, the correlation between the key prognostic RNA methylation regulators and the bile acid metabolism related genes in protein level was calculated by Pearson's test.

Statistical analysis

All statistical analyses were performed using R (http://www.R-project.org). The ROC curve and the area under the curve (AUC) were quantified using the "survivalROC" and the "timeROC" R packages. Kruskal-Wallis test and One-way ANOVA test were used to compare the difference among three or more groups. The statistical significance of two sample groups was estimated by the Wilcox test or the Student t-test. The forest plot was depicted using the Sangerbox tools, a free online platform for data analysis (http://www.sangerbox.com/tool). The Chi-square test was used to analyze the correlation between risk score and the clinicopathological parameters. Pearson's correla-

tion analysis was used to compute the correlation coefficients. P<0.05 was considered statistically significant.

Results

Landscape of gene expression and genetic variation of RNA methylation regulators in HCC

A total of 48 RNA methylation regulators, including 9 m6A writers, 2 m6A erasers, 13 m6A readers, 4 m1A writers, 2 m1A erasers, 3 m1A readers, 12 m5C writers, 4 m5C erasers and 2 m5C readers, were identified in this study through systematic literature search [7, 15, 16, 21]. Among them, ALKBH acts as the eraser for both m1A and m5C, while YTHDC1, YTHDF1, YTHDF2 and YTHDF3 act as the readers for both m6A and m1A (**Figure 1A**). **Figure 1B** summarized the top 20 incidences of somatic mutations of these 48 RNA methylation regulators in HCC. Among 364 samples, 60 samples had mutations in RNA methylation regulators, with a frequency of 16.48%. TET1 exhibited the highest somatic mutation rate (2%), followed by DNMT3A, HNRNPC, LRPPRC, DNMT1, FMR1, HNRNPA2B1, TET2/3, YTHDC1/2, ZC3H13, IGF2BP3, NSUN4, TRMT10C, WTAP and YTHDF1 with 1% mutation frequency. The other regulators did not exhibit any mutation in HCC samples. These results suggested that the somatic mutation frequency of RNA methylation regulators was low in HCC. Since copy number variation (CNV) is prevalent in RNA methylation regulators, we analyzed the CNV of RNA methylation regulators in these samples. We found that regulators, such as ALYREF, VIRMA, HNRNPC, METTL3, YTHDF3, IGF2BP2, DNMT3A, NSUN2, YTHDF1 and TRMT61B, showed gain of CNV in most cases, while other regulators, such as ZC3H13, TRMT61A, METTL16, YTHDF2, ALKBH1, WTAP, TET2, YBX1, NSUN4 and DNMT1, were mainly characterized by loss of CNV (**Figure 1C**). **Figure 1D** showed the chromosome location of these CNV.

In addition, we compared the mRNA levels of RNA methylation regulators between normal and HCC samples and found that the occurrence of CNV might be an important factor perturbating the expression of the RNA methylation regulators. RNA methylation regulators, such as ALYREF, HNRNPC, METTL3, YTHDF3, IGF2BP2, DNMT3A, NSUN2 and YTHDF1, that had gains of CNV expressed at markedly higher level in HCC tissues than in normal tissues (**Figure 1E**). Notably, the expression of most of these regulators was significantly higher in the late stages of HCC patients than in early stages of HCC patients (**Figure 1F**). Consistently, the gene expression and protein level of most of these regulators were also found significantly elevated in HCC tissues, especially in the late stages of HCC tissues, in ICGA and CPTAC cohorts (Figure S2). These results presented the changes in the expression landscape of RNA methylation regulators between normal liver and HCC tissues, as well as among various tumor stages, indicating that the upregulation of RNA methylation regulators played a vital role in the initiation and progression of HCC.

Identification of RNA methylation regulators with prognostic value

Univariate Cox regression was conducted for 43 regulators that had expression data. The results showed that 33 of the 43 regulators were markedly related to the overall survival (OS) of HCC patients (P<0.05) and were thus identified as prognostic RNA methylation regulators. The list of these 33 RNA methylation regulators was YTHDF1/2/3, TRMT6/61A/61B, TRMT10C, NSUN2/3/4/5, ALYREF, LRPPRC, KIAA1429, HNRNPC, DNMT3A, DNMT1, HNRNPA2B1, ELAVL1, WTAP, METTL3, ALKBH1, RBM15/15B, IGF2BP1/2/3, DNMT3B, TET3, YBX1, NOP2, CBLL1 and YTHDC1. Furthermore, we found that all these 33 regulators were associated with the poor prognosis of HCC and were positively correlated with each other (**Figure 2A**).

Construction of a prognostic RNA methylation regulators-based classifier

A total of 7 regulators (ALYREF, IGF2BP1, IGF2BP2, TRMT10C, TRMT61A, YTHDF2 and NSUN5) were selected as the most significant prognostic biomarkers based on the LASSO Cox regression analysis results (**Figure 2B**). The coefficient of each biomarker was also derived from the LASSO algorithm (**Figure 2C**).

We divided the patients into low- and high-risk group by using the cutoff value of the median risk score that was calculated by formula described above. When examining the gene expression of these 7 regulators in the low- and

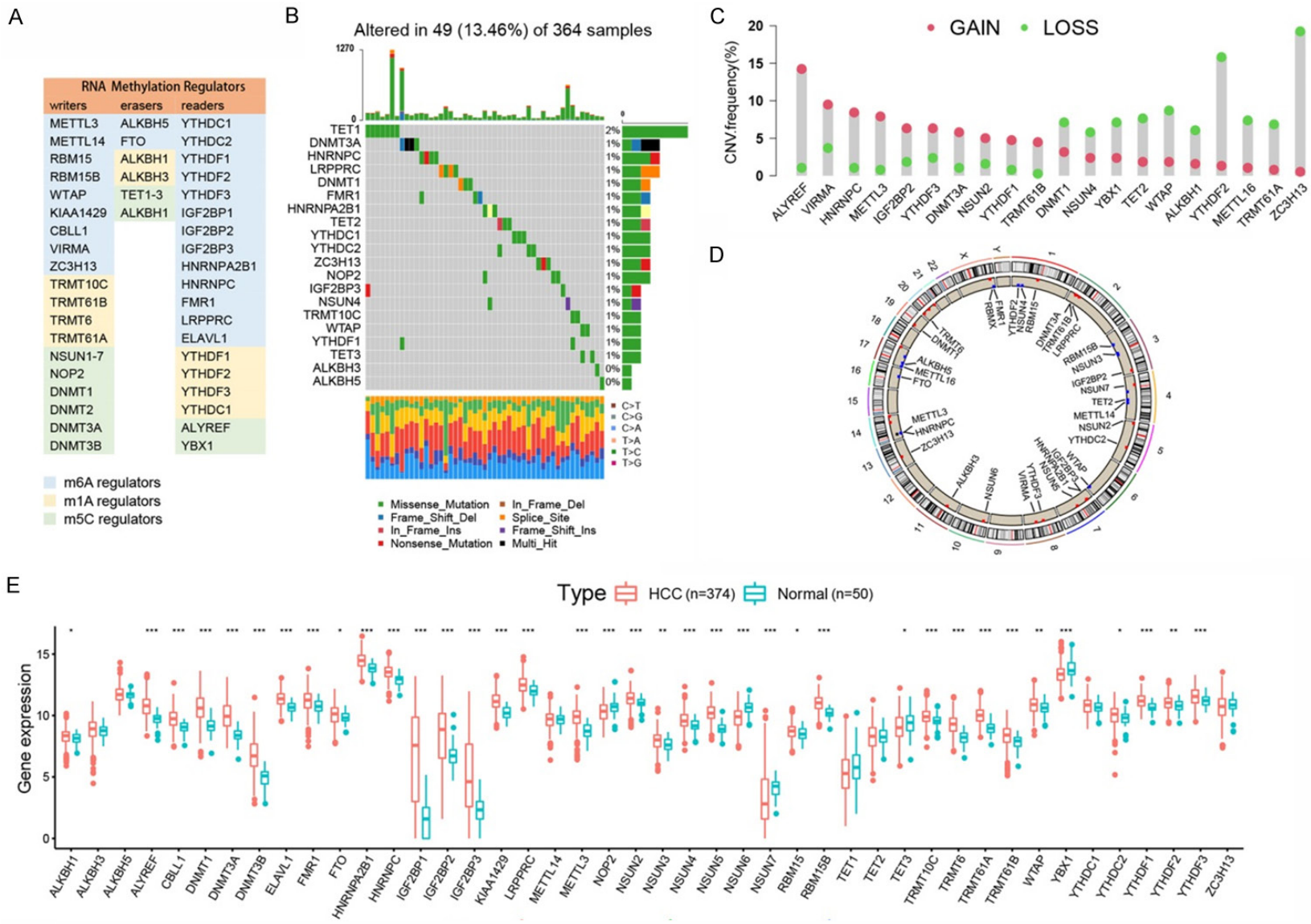
A
RNA Methylation Regulators
writers
erasers
readers
METTL3
METTL14
RBM15
RBM15B
WTAP
KIAA1429
CBLL1
VIRMA
ZC3H13
TRMT10C
TRMT61B
TRMT6
TRMT61A
NSUN1-7
NOP2
DNMT1
DNMT2
DNMT3A
DNMT3B
ALKBH5
FTO
ALKBH1
ALKBH3
TET1-3
ALKBH1
YTHDC1
YTHDC2
YTHDF1
YTHDF2
YTHDF3
IGF2BP1
IGF2BP2
IGF2BP3
HNRNPA2B1
HNRNPC
FMR1
LRPPRC
ELAVL1
YTHDF1
YTHDF2
YTHDF3
YTHDC1
ALYREF
YBX1
m6A regulators
m1A regulators
m5C regulators
B
Altered in 49 (13.46%) of 364 samples
C>T
C>G
C>A
T>A
T>C
T>G
Missense_Mutation
Frame_Shift_Del
In_Frame_Ins
Nonsense_Mutation
In_Frame_Del
Splice_Site
Frame_Shift_Ins
Multi_Hit
C
GAIN
LOSS
CNV.frequency(%)
D
E
Type
HCC (n=374)
Normal (n=50)
Gene expression

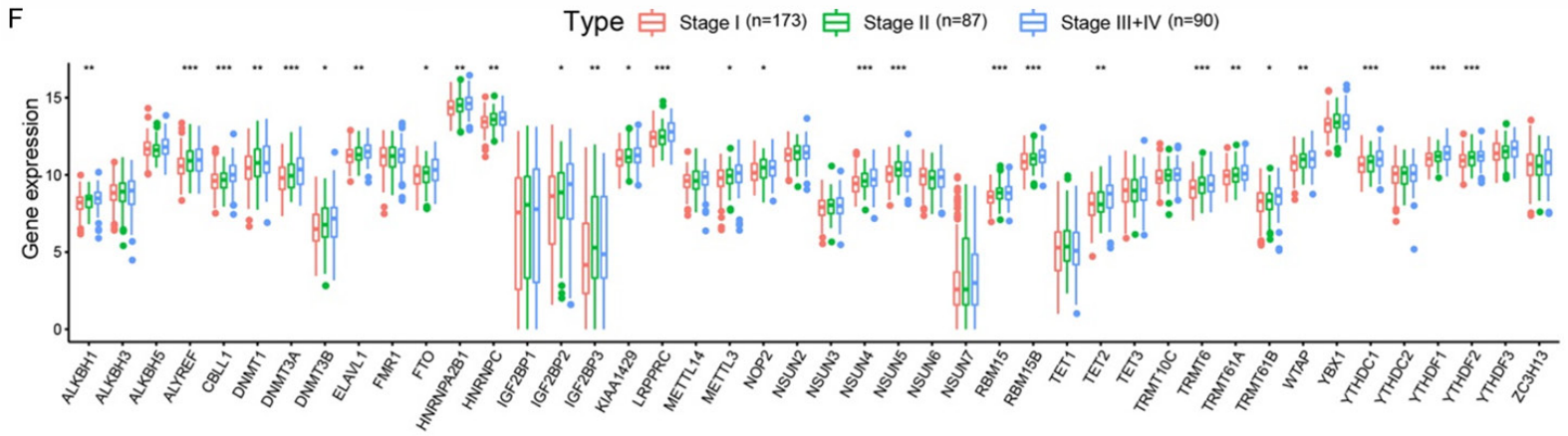

Figure 1. Expression and genetic landscapes of RNA methylation regulators in hepatocellular carcinoma (HCC). A. Members of RNA methylation (m6A, m1A, and m5C) regulators ("writers", "erasers" and "readers"). B. Top 20 somatic mutations of RNA methylation regulators in the TCGA cohort. Each column stood for a patient with an RNA methylation regulator mutation, and the upper panel shows the tumor mutation burden. The mutation frequency of each regulator was listed on the right of the columns. The barplot in the right showed the proportion of each variant type. The stacked barplot below showed a fraction of conversions in each sample. C. The top 20 CNV variation frequency of RNA methylation regulators in TCGA cohort. The height of the column stood for the alteration frequency. The blue dot stood for the deletion frequency, while the red dot stood for the amplification frequency. The right barplot shows the proportion of each variant type. The stacked barplot below shows the proportion of DNA base conversions in each sample. C. The CNV variation frequency of RNA methylation regulators in TCGA cohort. The height of the column stood for the alteration frequency. The blue dot stood for the deletion frequency, while the red dot stood for the amplification frequency. D. The location of CNV alteration of RNA methylation regulators on 23 chromosomes. E. Expression levels of RNA methylation regulators in HCC and adjacent normal tissues by Wilcox test. F. Expression levels of RNA methylation regulators in different tumor stages of HCC by Kruskal-Wallis test. *P<0.05; **P<0.01; ***P<0.001. CNV: copy number variations; TCGA: The Cancer Genome Atlas.

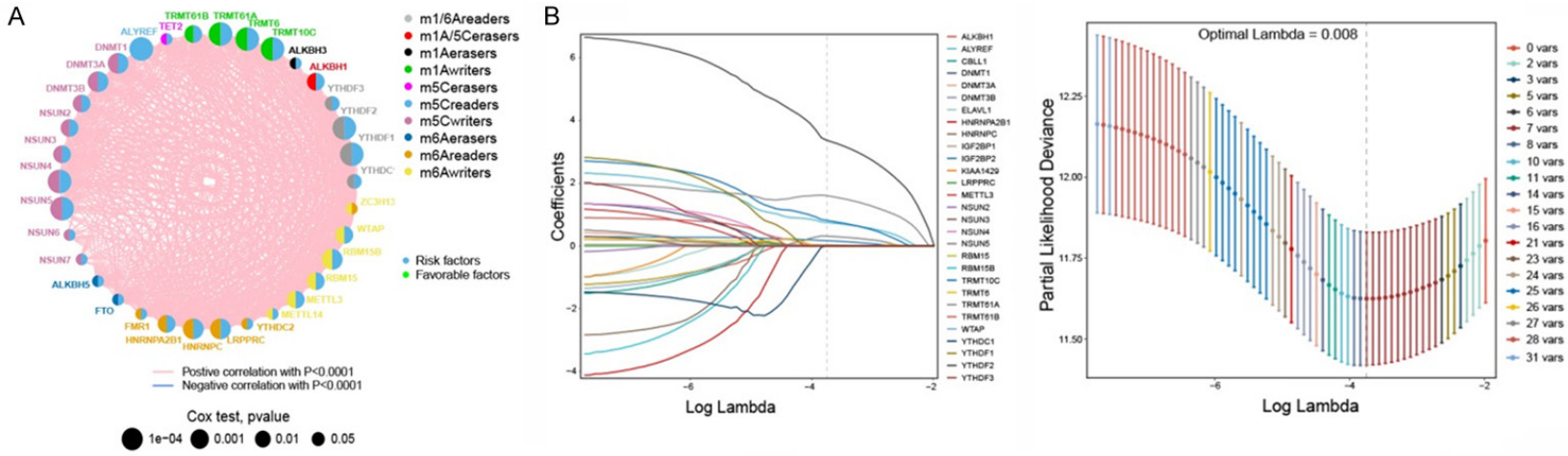

C

Symbol	Univariate Cox regression analysis			LASSO Coefficient
	HR	95%CI	P-value	
ALYREF	1.438	1.200-1.723	0.000	0.670
IGF2BP1	1.056	1.008-1.105	0.019	0.022
IGF2BP2	1.112	1.036-1.193	0.003	0.129
TRMT10C	1.805	1.376-2.367	0.000	0.689
TRMT61A	1.728	1.346-2.217	0.000	1.465
YTHDF2	2.183	1.592-2.994	0.000	3.108
NSUN5	1.632	1.285-2.074	0.000	0.265

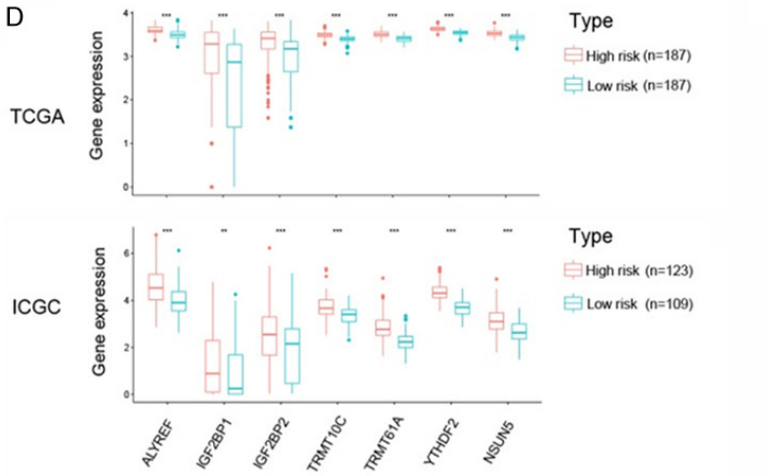

Figure 2. Construction of RNA methylation regulators-based prognostic classifier. A. The interaction between RNA methylation regulators in HCC. The circle size stood for the effect of each regulator on the prognosis of HCC, and the range of values were P<0.0001, P<0.001, P<0.01, and P<0.05, respectively. Green in the right of the circle stood for favorable factors of prognosis; Blue in the right of the circle stood for risk factors of prognosis. The lines linking regulators show their interactions, in which a negative correlation is marked with blue and a positive correlation with pink. The different types of the regulators are marked with different colors in the left of the circle. B. Results of the LASSO Cox regression screened 7 regulators that are essential for the prognosis of HCC. The left panel was the shrinkage profile of LASSO coefficients. It represented the relationship between the logarithm of lambda and coefficients of every gene. Each curve represented a coefficient (labeled on the right). The right panel was the cross-validation plot of LASSO, it represented the relationship between the logarithm of lambda and the partial likelihood deviance (or mean square error). The vertical dashed line in the figure represented the log lambda of the minimum partial likelihood deviance. C. The HR and coefficient of the 7 regulators in the prognostic classifier. D. Gene expression levels of all 7 regulators of the classifier in the high- and low-risk groups from the TCGA and ICGC cohorts. *P<0.05; **P<0.01; ***P<0.001. HR: hazard ratio.

Table 1. Correlations between risk score of the RNA methylation regulators-based classifier with clinicopathological parameters in the TCGA cohort

Parameters	TCGA cohort			
	High risk	Low risk	X^2	P
Age (y)			0.003	0.995
<60	84	85		
≥60	102	102		
Gender			0.559	0.439
Male	123	130		
Female	64	57		
Child grade			0.001	0.980
A	89	130		
B and C	9	13		
BMI			5.486	**0.019**
<28	125	118		
≥28	35	59		
Histologic grade			4.831	**0.028**
1-2	106	127		
3-4	78	58		
pT			9.887	**0.002**
1-2	127	151		
3-4	60	33		
pN			1.076	0.300
0	124	130		
1	3	1		
pM			0.008	0.929
0	128	140		
1	2	2		
Tumor stage			10.928	**0.001**
1-2	115	145		
3-4	58	32		

Bold values are statistically significant.

high-risk group, we found that the mRNA levels of all 7 regulators were significantly higher in the high-risk group than in the low-risk group in both TCGA and ICGC cohorts, further supporting their potential application as prognostic biomarkers (**Figure 2D**).

Correlation between the classifier and the clinicopathologic characteristics

As shown in **Table 1**, the clinical parameters of BMI (χ^2=5.468, P=0.019), histologic grade (χ^2=4.831, P=0.028), pathologic T (pT) (χ^2=9.887, P=0.002), and tumor stage (χ^2=10.928, P=0.001) were significant different between the low- and high-risk group.

Prognostic value of the classifier for assessing the overall survival of HCC patients

We further evaluated the prognostic significance of the classifier we identified above. As shown in **Figure 3A**, **3B**, patients in the high-risk group had a shorter OS time (P=1.338×10^{-5}) and recurrence-free survival (RFS) time (P=5.886×10^{-3}) in the TCGA cohort by Kaplan-Meier test. Moreover, the Area under the Curves (AUCs) for 1-, 3-, and 5-year OS were 0.759, 0.704 and 0.719 in the TCGA cohort, respectively (**Figure 3D**). More importantly, the predictive ability of the classifier was superior to tumor grade (TNM stage) and histologic grade, the two well-defined, major risk factors for patient prognosis.

To determine the robustness of this classifier, we compared the prognosis of the HCC patients in low- and high-risk group from the ICGC cohort based on the classifier. As shown in **Figure 3C**, patients in the high-risk group had a poor prognosis (P=2.86×10^{-3}) in the ICGC cohort. In addition, in the ICGC cohort, the AUCs for 1-, 3-, and 5-year OC were 0.727, 0.686 and 0.639, respectively (**Figure 3E**).

Moreover, we used the proteomics data from CPTAC and the microarray data from GEO database to validate our classifier. Integrating the protein level into the formula, we calculated and set a new median cutoff value to predict the prognosis of HCC in CTPAC cohort. As shown in Figure S3A, we found the protein levels of the 7 regulators were also upregulated in high-risk HCC samples. Patients in the high-risk group had a poor prognosis (P=1.179×10^{-2}) in the CTPAC cohort (Figure S3B). Similarly, we calculated and set a new median cutoff value to predict the prognosis of HCC in GSE54236 cohort. Consistently, as shown in Figure S3C, most of the 7 regulators were also upregulated in high-risk HCC samples, and the risk score had significantly negative correlation with the survival time (R=-0.47, P=9.8×10^{-6}) of HCC patients (Figure S3D). These results showed that our classifier performed equally well in different datasets we examined, which further demonstrated the predictive power and the reliability of our classifier for HCC prognosis.

The results of univariate and multivariate Cox regression analysis further confirmed the prognostic significance of the classifier and showed

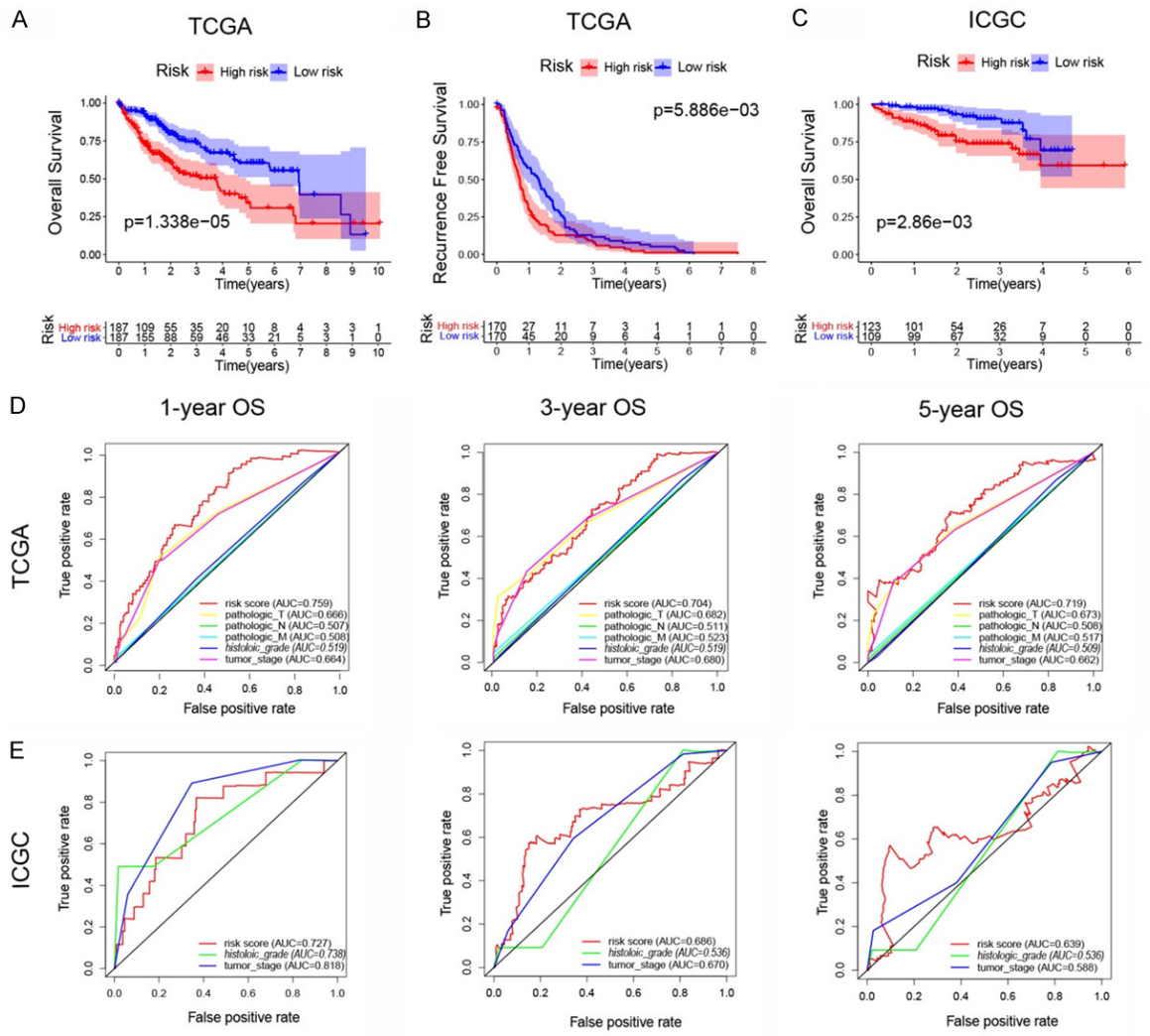

Figure 3. The prognostic value of the RNA methylation-based classifier. Kaplan-Meier survival analysis of OS (A) and recurrence-free survival (B) between the high- and low-risk patients from the TCGA cohort. Kaplan-Meier survival analysis of OS between the high- and low-risk patients from the ICGC cohort of HCC (C). The time-dependent ROC for 1-, 3-, and 5-year OS predictions for the classifier in comparison with clinical parameters in the TCGA (D) and ICGC (E) cohorts. OS: overall survival.

that the risk score based on the classifier was an independent risk factor for the survival of HCC patients (**Figure 4A**). Importantly, our classifier also performed better than other previously published classifiers in predicting long-term HCC prognosis. As shown in **Figure 4C**, the AUC of our classifier for 1-yar OS was higher than other classifiers constructed based on the genes associated with HIF-1 signaling [32], RNA binding protein (RBP) [33], metabolism [34], immune response [35], ferroptosis [36], a 6-gene-based classifier [37] and m6A regulators [38]. For 3-year OS, the AUC of our classifier was higher than the classifiers using genes related to immune response, ferroptosis, metabolism, a 6-gene, mitochondrial [39] and m6A-based classifier. Similar superior performance was also observed with our classifier for 5-year OS compared with other classifiers that were related to immune response, ferroptosis, RBP, metabolism, a 6-gene, mitochondrial and m6A-based classifier. Moreover, as shown in **Figure 4D**, the AUCs of our classifier were superior to others in predicting the long-term OS (more than 4 years). Collectively, these results suggested that our RNA methylation regulator-based classifier is a useful prognostic tool for categorizing patients with HCC.

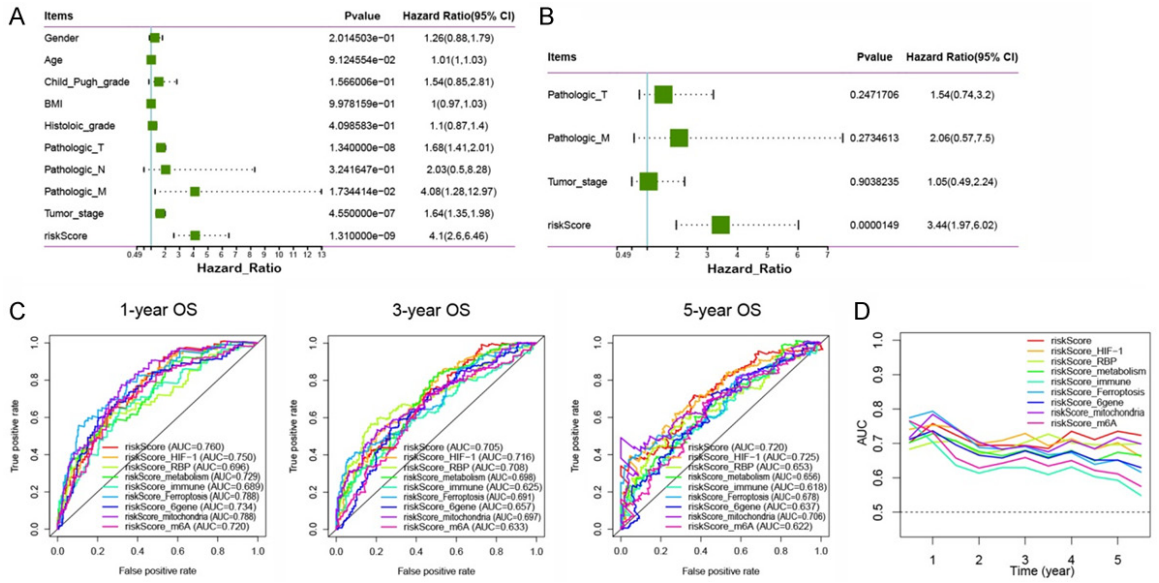

Figure 4. The independent prognostic significance of the classifier. A and B. Univariate and multivariate Cox regression analyses of the classifier with OS in the TCGA cohort. C and D. The time-dependent ROC for 1-, 3-, and 5-year OS predictions for the classifier in comparison with other classifiers published previously.

Identification of differentially expressed genes (DEGs) and functional annotation between high- and low-risk groups

To understand the differences in the molecular and biological processes between the high- and low-risk groups, we investigated 1575 DEGs (1537 upregulated and 38 downregulated) using the "limma" package (**Figure 5A**; Table S2). Next, we conducted a functional annotation analysis by Metascape database to reveal the different biological processes between the two groups. As shown in **Figure 5B**, the upregulated genes were most enriched in the processes associated with the cell cycle, e.g., mitotic cell cycle process, meiotic cell cycle, positive regulation of cell cycle, regulation of mitotic nuclear division, nuclear division, and regulation of cell division. In contrast, the downregulated genes were most enriched in metabolic processes, e.g., fatty acid metabolism, carbon metabolism, lipid modification, triglyceride metabolic process, bile secretion, farnesoid X receptor pathway, alpha-amino acid metabolic process, and monocarboxylic acid metabolic process.

To identify the altered biological processes between normal and HCC samples as well as among HCC samples, we conducted the GSVA analysis. As shown in **Figure 5C**, in line with the above results, many metabolism pathways, including primary bile acid biosynthesis, glycine serine and threonine metabolism, fatty acid metabolism, butanoate metabolism, beta alanine metabolism, valine leucine and isoleucine degradation, propanoate metabolism, tryptophan metabolism, retinol metabolism, metabolism of xenobiotics by cytochrome p450, tyrosine metabolism, arginine and proline metabolism and oxidative phosphorylation, were significantly downregulated in HCC samples compared with normal liver tissues. Moreover, these metabolism pathways were much lower in high-risk HCC than in low-risk HCC. On the other hand, cell cycle and RNA degradation pathways were significantly upregulated in HCC samples and expressed at much higher level in the high-risk group than in the low-risk group. Together, these results indicate that the regulators of RNA methylation negatively regulate the metabolic processes in HCC.

Metabolic characteristics among different RNA methylation modification patterns

To determine the alteration of metabolic processes in HCC among different RNA methylation modification patterns, we conducted an unsupervised clustering analysis by the "ConsensusClusterPlus" package based on the expression of the RNA methylation regulators. At

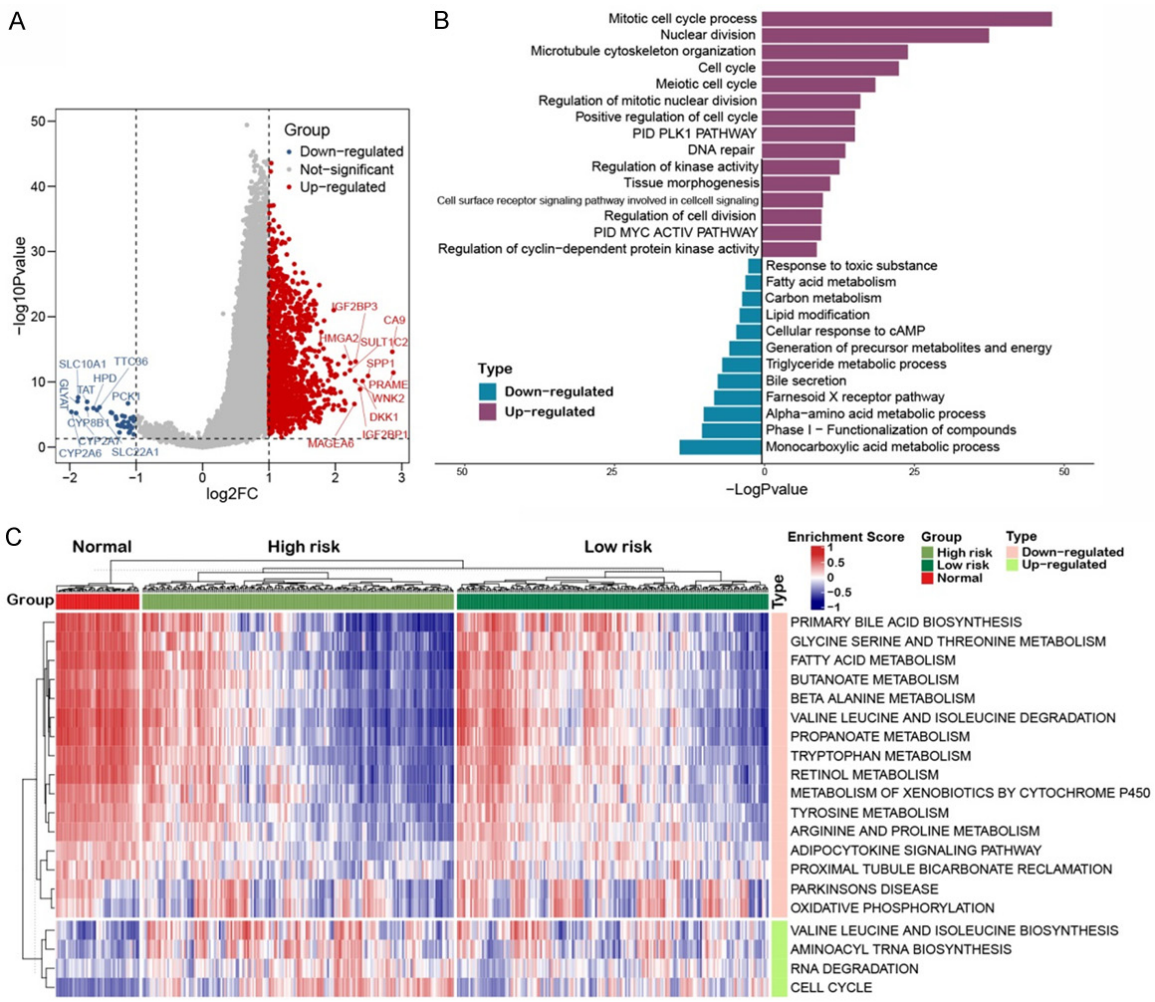

Figure 5. Functional enrichment analysis between high- and low-risk groups. A. The volcano plot showed DEGs between high- and low-risk groups, and red stood for upregulated DEGs and blue stood for downregulated DEGs. B. Barplot was used to visualize the result of functional enrichment analysis of the DEGs, and purple stood for activated pathways and blue stood for inhibited pathways. C. GSVA analysis showed the activation states of biological pathways based on the KEGG database in normal, low- and high-risk HCC samples. DEGs: differentially expressed genes; KEGG: Kyoto Encyclopedia of Genes and Genomes.

the end, as shown in **Figure 6A**, **6B**, three distinct clusters were identified in the TCGA cohort: cluster 1 with 132 cases in, cluster 2 with 124 cases, and cluster 3 with 118 cases. Cluster 2 had the highest risk score, while cluster 1 had the lowest risk score (**Figure 6C**). Kaplan-Meier analysis also showed that patients with the highest risk score in cluster 2 had the worst prognosis, and patients in cluster 1 had the best prognosis. Furthermore, we explored the differences in the RNA methylation regulator modification patterns among these clusters. As shown in **Figure 6D**, consistent with the results based on the risk score, cluster 2 had the highest expression level of most RNA methylation regulators, while cluster 1 had the lowest regulator expression level.

Furthermore, we performed GSVA analysis of 186 KEGG pathways to depict the metabolism characteristics of each cluster. As shown in **Figure 7A**, cluster 1 was hyperactive in carbohydrate, lipid, and amino acid metabolism, while cluster 2 showed the opposite expression, lower in these metabolic processes. The univariate Cox regression analysis showed that the activities of some metabolic processes were protective for HCC prognosis; these processes included linoleic acid metabolism, arachidonic acid metabolism, primary bile acid bio-

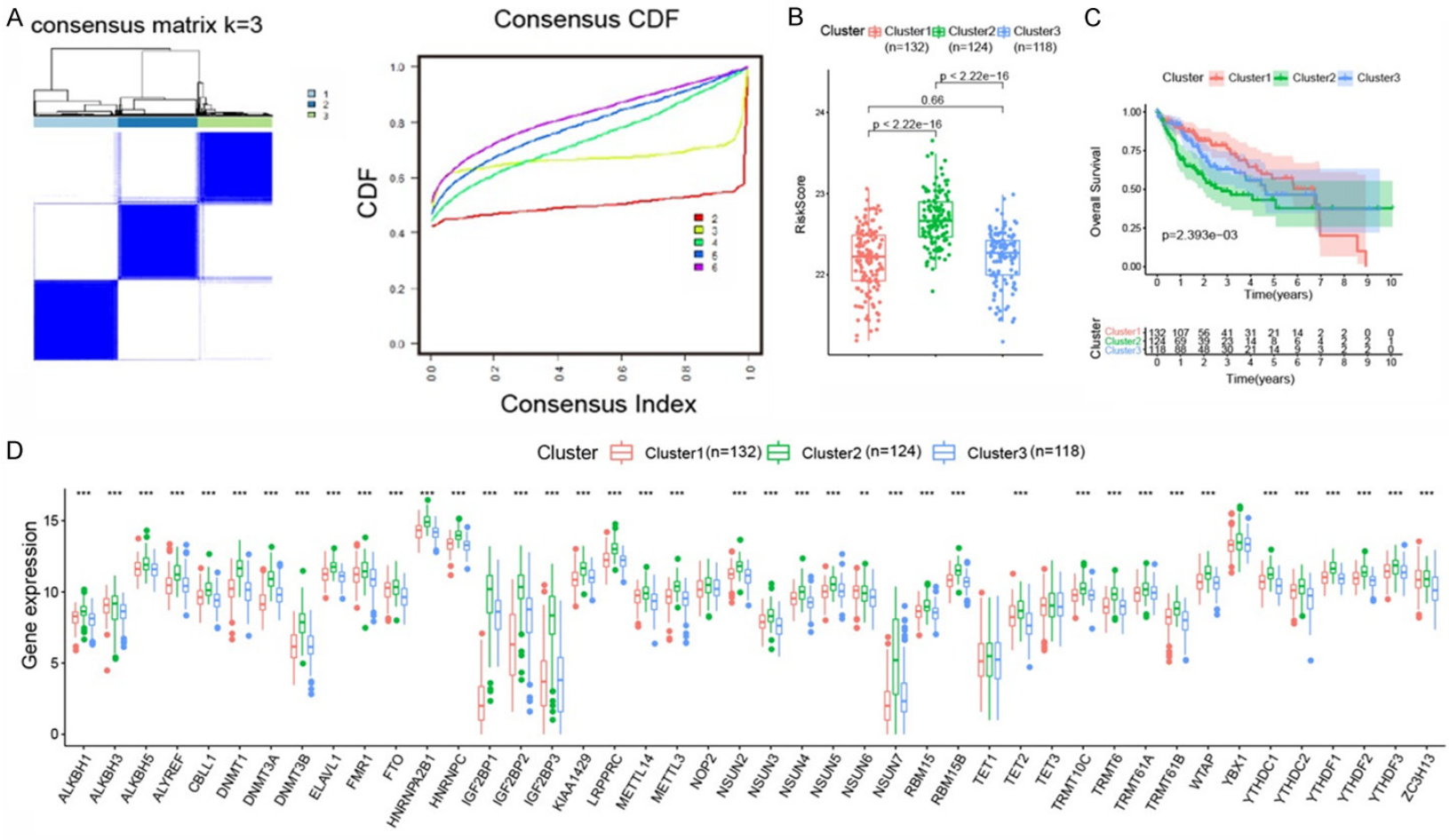
A
consensus matrix k=3
Consensus CDF
CDF
Consensus Index
B
Cluster Cluster1 (n=132) Cluster2 (n=124) Cluster3 (n=118)
p < 2.22e−16
0.66
p < 2.22e−16
RiskScore
C
Cluster Cluster1 Cluster2 Cluster3
Overall Survival
p=2.393e−03
Time(years)
Cluster
Time(years)
D
Cluster Cluster1 (n=132) Cluster2 (n=124) Cluster3 (n=118)
Gene expression
ALKBH1 ALKBH3 ALKBH5 ALYREF CBLL1 DNMT1 DNMT3A DNMT3B ELAVL1 FMR1 FTO HNRNPA2B1 HNRNPC IGF2BP1 IGF2BP2 IGF2BP3 KIAA1429 LRPPRC METTL14 METTL3 NOP2 NSUN2 NSUN3 NSUN4 NSUN5 NSUN6 NSUN7 RBM15 RBM15B TET1 TET2 TET3 TRMT10C TRMT6 TRMT61A TRMT61B WTAP YBX1 YTHDC1 YTHDC2 YTHDF1 YTHDF2 YTHDF3 ZC3H13

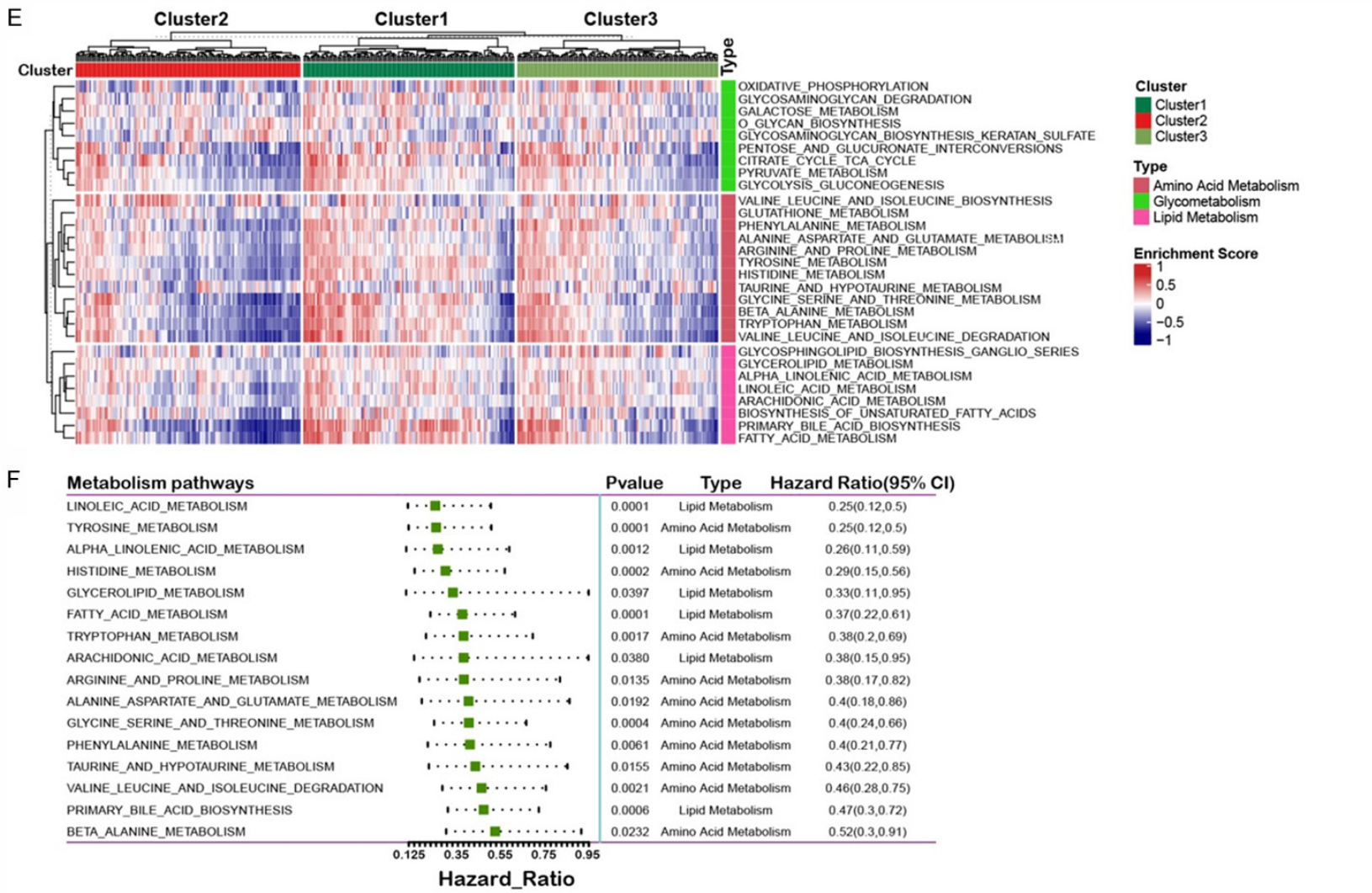

Figure 6. Unsupervised clustering based on RNA methylation regulators. A. Heatmaps of the consensus matrices for k=3. B. Differences of the risk score among 3 clusters in the TCGA cohort by Wilcox test. C. Kaplan-Meier analysis of overall survival among 3 clusters in the TCGA cohort. D. Differences of the expression of RNA methylation regulators among 3 clusters in the TCGA cohort by Kruskal-Wallis test. E. GSVA analysis showed the activation states of metabolic pathways based on the KEGG database among 3 clusters in the TCGA cohort. F. Univariate Cox regression analysis of the activation of metabolic pathways with OS in the TCGA cohort. *P<0.05; **P<0.01; ***P<0.001.

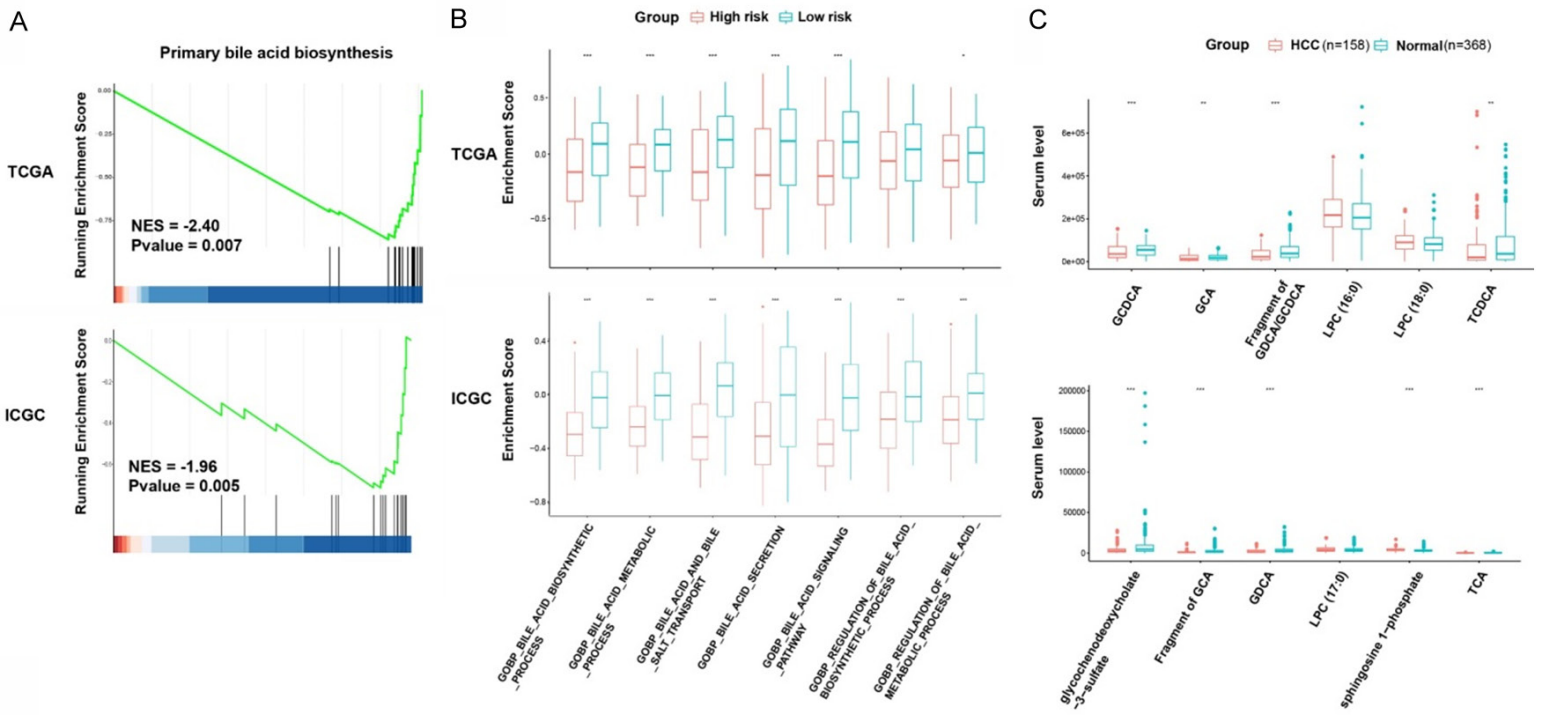

D

Chenodeoxycholic acid			Cholic acid			Dehydrocholic acid			Taurodeoxycholic acid			Taurocholic acid		
Name	Score	Type	Name	Score	Type	Name	Score	Type	Name	Score	Type	Name	Score	Type
GW-9662	99.9	PPAR receptor antagonist	LY-364947	98.65	TGF beta receptor inhibitor	GSK -461364	99.12	PLK inhibitor	nobiletin	99.35	MEK inhibitor	geranylgeraniol	99.9	Farnesyltransferase inhibitor
pifithrin	99.74	Interleukin receptor antagonist	valproic -acid	98.44	HDAC inhibitor	imatinib	98.55	BCR -ABL kinase inhibitor	NU-1025	98.6	PARP inhibitor	vicriviroc	99.15	CC chemokine receptor antagonist
decitabine	99.64	DNA methyltransferase inhibitor	GW-9662	98.12	PPAR receptor antagonist	AG -490	98.44	EGFR inhibitor	zebularine	97.94	DNA methyltransferase inhibitor	razoxane	98.44	Chelating agent
erlotinib	99.48	EGFR inhibitor	ellipticine	97.23	Topoisomerase inhibitor	linsitinib	97.57	IGF -1 inhibitor	XMD-892	97.66	MAP kinase inhibitor	gefitinib	97.85	EGFR inhibitor
KU -55933	98.44	ATM kinase inhibitor	AICA -ribonucleotide	96.39	AMPK activator	pirfenidone	97.5	TGF beta receptor inhibitor	axitinib	97.49	PDGFR receptor inhibitor	cediranib	96.93	KIT inhibitor
bosutinib	98.17	ABL inhibitor	veliparib	95.93	PARP inhibitor	AICA -ribonucleotide	97.28	AMPK activator	palbociclib	97.21	CDK inhibitor	tyrphostin -AG -1296	95.49	FLT3 inhibitor
sunitinib	96.11	PLK inhibitor	rucaparib	94.08	PARP inhibitor	tipifarnib	96	Farnesyltransferase inhibitor	BMS -754807	97.02	IGF -1 inhibitor	sunitinib	93.55	PLK inhibitor
masitinib	95.06	KIT inhibitor	orantinib	93.33	FGFR inhibitor	linifanib	94.23	PDGFR receptor inhibitor	NU-7441	96.48	DNA dependent protein kinase inhibitor	KU -55933	93.31	ATM kinase inhibitor
pyrazolanthrone	93.51	JNK inhibitor	sunitinib	93.29	FLT3 inhibitor	lestaurtinib	92.81	FLT3 inhibitor	tubacin	93.5	HDAC inhibitor	4,5-dianilinophthalimide	93.05	EGFR inhibitor
gefitinib	90.02	EGFR inhibitor	rottlerin	91.06	MAP kinase inhibitor	tivozanib	92.49	VEGFR inhibitor	tandutinib	90.38	FLT3 inhibitor	lestaurtinib	91.45	FLT3 inhibitor

Figure 7. The alteration and potential therapeutic effect of bile acid metabolism on HCC. A. The enrichment of primary bile acid biosynthesis pathway between high- and low-risk HCC by GSEA analysis in both TCGA and ICGC cohorts. B. Differences of genesets associated with bile acid metabolism from GO-BP gene signature between high- and low-risk HCC samples by GSVA analysis in both TCGA and ICGC cohorts by Student t test. C. Differences of serum metabolites between normal and HCC patients by Wilcox test. D. The anti-tumor agents with similar gene expression patterns (connective score >90) with bile acids. GCDCA: glycochenodeoxycholic acid; GCA: glycocholic acid; GDCA: glycodeoxycholic acid; TCDCA: taurochenodeoxycholic acid; TCA: taurocholic acid; GO-BP: gene ontology-biological process; LPC: lysophosphatidylcholine. *P<0.05; **P<0.01; ***P<0.001.

synthesis, fatty acid metabolism, tyrosine metabolism and histidine metabolism.

To further validate the metabolic alteration patterns among different RNA methylation clusters, we used another cohort, ICGC, to conduct unsupervised clustering analysis based on the expression of the RNA methylation regulators and to perform GSVA enrichment analysis. Patients in ICGC were divided into 3 clusters, with 106 samples in cluster 1, 21 samples in cluster 2, and 105 samples in cluster 3 (Figure S4A). Consistent with the results from the TCGA cohort, cluster 2 with the highest risk score had the highest expression of RNA methylation regulators and the worst prognosis, while cluster 3 was the opposite (Figure S4B-D). In addition, cluster 2 had reduced activity in carbohydrate, lipid, and amino acid metabolism. And the activity of some metabolic processes (e.g., linoleic acid metabolism, arachidonic acid metabolism, fatty acid metabolism, primary bile acid biosynthesis, tyrosine metabolism and histidine metabolism) had protective function for HCC prognosis in ICGC cohort too (Figure S4E, S4F). These observations further supported our conclusion that RNA methylation regulators negatively mediated the metabolic processes in HCC. The suppression of metabolisms by RNA methylation regulators may attribute to the unfavorable prognosis in the high-risk group.

Alteration and potential therapeutic effect of bile acids on HCC

Our previous study has revealed the prognostic role of the primary bile acid biosynthesis pathway in HCC [39]. Given that bile acids are liver-specific metabolic substances, and primary bile acid synthesis pathway is the most downregulated metabolism process in HCC samples, we further investigated the dysregulation and the functional importance of bile acids in HCC. As shown in **Figure 7A**, the primary bile acid biosynthesis pathway was downregulated mostly in the high-risk group in both TCGA and ICGC cohorts by GSEA analysis. Furthermore, other bile acid metabolic processes derived from gene ontology-biological process (GO-BP) gene signatures were also downregulated in the high-risk group (**Figure 7B**). In addition, the levels of serum bile acids, including GCDCA, GCA, Fragment of GDCA/GCDCA, TCDCA, Fragment of GCA, GDCA and TCA, were significantly lower in HCC patients than in normal patients (**Figure 7C**). These results suggested that these bile acids might inhibit the occurrence and progression of HCC. To prove this, we used the approach of screening similar compounds in the cMap database to indirectly explore the anti-tumorigenic effects of bile acids. As shown in **Figure 7D**, bile acids, such as CDCA, CA, DCA, TDCA and TCA, exhibited similar (connective score >90) gene expression regulation patterns to other well-defined anti-tumor compounds (e.g., erlotinib, bosutinib, sunitinib, masitinib, gefitinib, veliparib, rucaparib, etc.), indicating the functional similarity between these bile acids and other anti-tumor compounds. In summary, the results above showed that bile acids metabolism was downregulated markedly in HCC, indicating the importance of bile acids in the progression, prognosis, and treatment of HCC.

Regulatory effects of RNA methylation regulators on bile acid metabolism genes

After identifying a negative regulation of bile acid metabolism by RNA methylation regulators, we sought to depict the regulatory network between RNA methylation regulators and bile acid metabolism genes. Firs, we reviewed the incidence of somatic mutation of 15 primary bile acid biosynthesis genes in HCC. Among 364 samples examined, 23 samples experienced gene mutations, with a frequency of 6.32%. ACOX2, CYP8B1, SCP2, AKR1D1 and CYP27A1 exhibited the highest mutation frequency of 1%, while HSD17B4 did not show any mutation in HCC samples (**Figure 8A**). The low somatic mutation frequency suggested

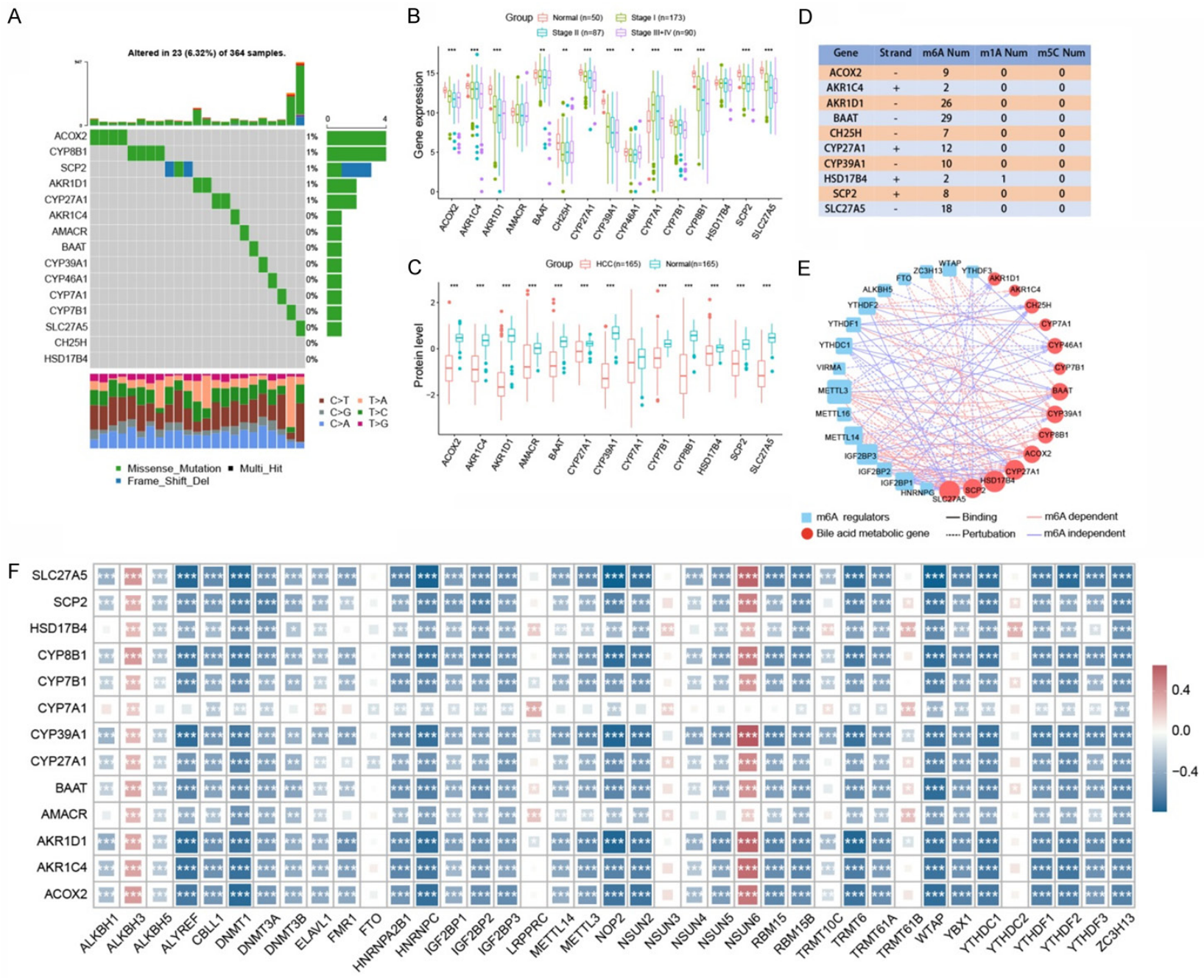
A
Altered in 23 (6.32%) of 364 samples.
ACOX2
CYP8B1
SCP2
AKR1D1
CYP27A1
AKR1C4
AMACR
BAAT
CYP39A1
CYP46A1
CYP7A1
CYP7B1
SLC27A5
CH25H
HSD17B4
C>T
C>G
C>A
T>A
T>C
T>G
Missense_Mutation
Multi_Hit
Frame_Shift_Del
B
Group
Normal (n=50)
Stage I (n=173)
Stage II (n=87)
Stage III+IV (n=90)
Gene expression
C
Group
HCC (n=165)
Normal(n=165)
Protein level
D
Gene | Strand | m6A Num | m1A Num | m5C Num
ACOX2 | - | 9 | 0 | 0
AKR1C4 | + | 2 | 0 | 0
AKR1D1 | - | 26 | 0 | 0
BAAT | - | 29 | 0 | 0
CH25H | - | 7 | 0 | 0
CYP27A1 | + | 12 | 0 | 0
CYP39A1 | - | 10 | 0 | 0
HSD17B4 | + | 2 | 1 | 0
SCP2 | + | 8 | 0 | 0
SLC27A5 | - | 18 | 0 | 0
E
m6A regulators
Bile acid metabolic gene
Binding
Pertubation
m6A dependent
m6A independent
F
0.4
0.0
−0.4

Figure 8. The regulation of bile acid metabolism pathways by RNA methylation regulators. A. Somatic mutations in primary bile acid biosynthesis genes in TCGA cohort. Each column stood for a patient with a gene mutation, and the upper panel shows the tumor mutation burden. The mutation frequencies of each regulator are listed in the right of the columns. The right barplot shows the proportion of each variant type. The stacked barplot below showed a proportion of DNA base conversions in each sample. B. Differences in the expression level of primary bile acid biosynthesis genes among normal and different stages of HCC in the TCGA cohort by Kruskal-Wallis test. C. Differences in the protein level of primary bile acid biosynthesis regulators between normal and HCC in the CPTAC cohort by Student t test. D. The number of RNA methylation sites in bile acid metabolic genes. E. The regulatory network between m6A regulators and bile acid metabolic genes. The blue square stood for m6A regulators, the red circle stood for bile acid metabolic genes. The solid line stood for the m6A regulators mediated target genes by "Binding manner", the dotted line stood for the m6A regulators mediated target genes by "Perturbation manner". The red line stood for the regulation of m6A regulators on target genes is m6A dependent, while the blue line is m6A independent. F. The correlation between the protein levels of RNA methylation regulators and bile acid metabolic regulators. *P<0.05; **P<0.01; ***P<0.001.

that the expression level of this gene was important for the activity of the primary bile acid synthesis pathway in HCC. As shown in **Figure 8B**, except for CYP7A1, all genes were downregulated in HCC compared to normal tissues. Moreover, the expression of BAAT, CYP27A1, CYP39A1, CYP7B1, CYP8B1 and SLC27A5 was decreased inversely with the increase of tumor stage. In addition, consistent with gene expression level, the protein levels of these bile acid biosynthesis regulators were downregulated markedly in HCC, except for CYP7A1 (**Figure 8C**). These results indicated a negative relationship between RNA methylation regulators and bile acid metabolism and that the downregulation of bile acid metabolism genes, especially BAAT, CYP27A1, CYP8B1 and SLC27A5, played a critical role in the tumorigenesis and poor prognosis of HCC.

We next explored the role of RNA methylation regulators on bile acid biosynthesis genes by analyzing the RNA methylation of these genes. As shown in **Figure 8D**, BAAT exhibited the most RNA methylation sites (29 m6A sites), followed by AKR1D1 (26 m6A sites), SLC27A5 (18 m6A sites) and CYP27A1 (12 m6A sites). The detailed information on RNA methylation sites was summarized in Table S3. Furthermore, we found that the relationship between m6A regulators and bile acid metabolism genes was complex. For example, METTL3 regulated the expression of ACOX2, BAAT, CYP39A1, CYP46A1 and SLC27A5 through a "binding manner"; the interaction between m6A regulators and target genes was suggested by CHIP-seq, CLIP-seq, RIP-seq and mass spectrometry. However, METTL3 also regulated the expression of AKR1C4, AKR1D1, BAAT, CYP27A1, CYP7A1, CYP8B1 and HSD17B4 through a "perturbation manner"; the interaction between m6A regulators and target genes was suggested by MeRIPseq, and RNA-seq. Besides, the regulation of METTL3 on ACOX2, BAAT, CYP39A1, CYP7A1, CYP8B1, HSD17B4, SCP2 and SLC27A5 was m6A dependent; the gene region of the target gene had 1 bp overlap with N6-Methyladenosin peak regions (**Figure 8E**). Since RNA methylation is one of the key mechanisms of post-transcriptional modification, which plays a crucial role in RNA translation and affects the biosynthesis of protein, we next explored the correlation between the protein level of RNA methylation regulators and the bile acid metabolism regulators. As shown in **Figure 8F**, most RNA methylation regulators were negatively correlated with bile acid metabolism regulators, except for ALKBH3, FTO, LRPPRC, NSUN6, TRMT61B and YTHDC2. These results indicated that the perturbation of RNA methylation was closely associated with the downregulation of bile acid metabolism, which might be related to the occurrence, development, and poor prognosis of HCC, providing a potential therapeutic target for HCC.

Discussion

In this study, for the first time, we constructed a 7 RNA methylation regulators-based prognostic classifier for HCC and validated its value in predicting the prognosis of HCC patients in several datasets. This classifier performed well and robustly predicted the prognosis of HCC patients from the TCGA, ICGC, and CTPAC cohorts. More importantly, the predictive ability of this classifier was superior to tumor grade (TNM stage) and histologic grade, the two commonly used risk factors for tumor prognosis [40, 41]. Our classifier was also better than other previously published classifiers in predicting long-term HCC prognosis.

All the 7 RNA methylation regulators in this classifier, ALYREF, IGF2BP1, IGF2BP2, TRMT-10C, TRMT61A, YTHDF2 and NSUN5, were risk-associated and overexpressed in the high-risk group. Both the gene expression and protein level of these regulators were significantly higher in HCC than in normal liver tissues, suggesting that these genes play important roles in the occurrence and progression of HCC. ALYREF is a "reader" of m5C, which serves as a specific m5C-binding protein and promotes mRNA export and post-transcriptional regulation [42, 43]. Wang et al. have reported that ALYREF drives glioblastoma (GBM) cell proliferation by stabilizing MYC mRNA and activating the Wnt/β-catenin signaling pathway, suggesting that ALYREF-MYC signaling may be a potential therapeutic target for GBM treatment [44]. Moreover, in bladder cancer, ALYREF has been found to promote bladder cancer cell proliferation by modulating PKM2-mediated glycolysis via direct binding to PKM2 mRNA and regulating its stability [45]. Recently, Nagy et al. have revealed that ALYREF forms a complex with MYCN and promotes neuroblastoma tumorigenesis through upregulating ubiquitin-specific protease 3 (USP3) expression [46]. Furthermore, consistent with our results, Xue et al. have reported that ALYREF is significantly upregulated in HCC tissues and HCC cell lines, and the expression of ALYREF is significantly correlated with both advanced tumor stages and poor prognosis [47]. However, the mechanism of the oncogenic effect of ALYREF on HCC is mainly unclear. IGF2BP1 and IGF2BP2 are two "readers" of m6A, which belong to the family of insulin-like growth factor 2 (IGF2) mRNA-binding proteins and regulate the localization, stability, or translation of their target RNAs through direct interaction [48]. Gutschner et al. first demonstrated the oncogenic role of IGF2BP1 on HCC through its interaction with c-MYC and MKI67 mRNAs to promote tumor progression [49]. In addition, IGF2BP1 has been reported to upregulate CD47 and contribute to sublethal heat treatment-induced HCC recurrence and metastasis [50]. IGF2BP1 is also known to facilitate the liver cancer stem cells phenotypes by promoting the stability of alpha-1,6-mannosylglycoprotein 6-beta-N-acetylglucosaminyltransferase (MGAT5) mRNA through elevating its m6A modification [51]. IGF2BP2 has also been found to promote the growth of HCC by targeting flap structure-specific endonuclease 1 (FEN1) through an m6A-dependent mechanism [52]. YTHDF2 is also a "reader" of m6A, which is involved in the development of various cancers, including HCC [53]. For example, the YTHDF2-dependent m6A of SOCS2 mRNA plays a vital role in METTL3-induced HCC progression [8]. In addition, YTHDF2 promotes the liver cancer stem cell phenotype and HCC metastasis by mediating the m6A methylation of OCT4 mRNA [54]. On the contrary, YTHDF2 can also function as a tumor suppressor in HCC. Hou et al. have reported that the deficiency of YTHDF2 promotes HCC cell growth, metastasis, inflammation, and vasculature remodeling through enhancing the decay of IL11 and serpin family E member 2 (SERPINE2) mRNAs [12]. TRMT-10C, TRMT61A and NSUN5 have been found significantly involved in the progression of various cancers [55-58]. However, to date, the role of these regulators in HCC has not been clearly defined.

In the present study, we found that the metabolic pathways associated with fatty acid, amino acid and carbohydrate metabolism were downregulated markedly in high-risk HCC patients, indicating that these metabolic processes play an important role in the progression of HCC. Furthermore, based on the expression of RNA methylation regulators, we defined 3 distinct RNA methylation modification clusters in HCC that were correlated with different metabolic patterns. The cluster with the highest risk score and highest expression level of RNA methylation regulators is the least active in carbohydrate, lipid, and amino acid metabolism. These results indicated that metabolic processes were the major targets of RNA methylation regulators in HCC.

Recently, increasing evidence has demonstrated the critical roles of RNA methylation regulators on metabolism. Li et al. found that METTL3 expression and m6A level increased in the liver of high-fat diet (HFD) mice, and the overexpression of METTL3 aggravated liver metabolic disorders and hepatogenous diabetes [59]. In contrast, YTHDC2 was markedly down-regulated in NAFLD patients, and the overexpression of liver YTHDC2 reduced liver steatosis and insulin resistance through binding to mRNA of lipogenic genes, thereby leads to decreasing their mRNA stability and inhibiting the expression of

lipogenic genes, including sterol regulatory element-binding protein 1c (SREBP1c), fatty acid synthase (FASN), stearoyl-CoA desaturase 1 (SCD1) and acetyl-CoA carboxylase 1 (ACACA1) [60]. FTO has been found to regulate carbohydrate metabolism via modulating the expression of forkhead box O1 (FOXO1) and activating transcription factor 4 (ATF4), which subsequently affects glucose-6-phosphatase (G6PC) expression in an m6A-dependent manner when exposed to pathological conditions. However, under physiological conditions, FTO regulates transcription factors, such as signal transducer and activator of transcription 3 (STAT3), CCAAT enhancer binding protein-β (C/EBP-β) and CAMP responsive element binding protein 1 (CREB1), and affects carbohydrate metabolism in an m6A-independent manner [61]. Furthermore, FTO also regulates lipid metabolisms through affecting cell cycle and increasing the m6A levels of cyclin A2 (CCNA2) and cyclin-dependent kinase 2 (CDK2) in a YTHDF2-dependent m6A manner [62]. As for the function of METTL3 in HCC, it has been reported that METTL3-mediated m6A modification leads to the elevation of LINC00958 via stabilizing its RNA transcript, thereby facilitating HCC lipogenesis and progression [63]. METTL3 also promotes glycolysis metabolism and improves the sensitivity to glycolytic stress in HCC, partially mediated by an m6A modification of HIF-1α mRNA [64, 65]. Similarly, ALYREF can directly bind to PKM2 mRNA and regulate its stability; thus, promote bladder cancer cell proliferation by PKM2-mediated glycolysis [45].

Another finding in our current study revealed that the processes of bile acid metabolism were markedly downregulated in the high-risk group HCC patients. The levels of serum bile acids, such as GCDCA, GCA, GDCA, Fragment of GDCA/GCDCA, TCDCA, Fragment of GCA and TCA, were also significantly decreased in HCC patients. Consistent with the recent study by Han et al., we also observed that the serum chenodeoxycholic acid (CDCA), TCA, GCA, TCDCA, GCDCA and deoxycholic acid (DCA) were significantly decreased in HCC patients, which might serve as biomarkers for the diagnosis of HCC (AUC >0.8) [66]. In addition, we found that CDCA, CA, DCA, TCDCA and TCA showed similar (connective score >90) expression patterns with some well-defined anti-tumor compounds, suggesting the potential anti-tumor capacity of these bile acids on HCC. Previous studies have shown that TCDCA, GCDCA, GCA and DCA induce reactive oxygen species (ROS) and cell apoptosis in liver cancer cells [67]. A high concentration of bile acids can induce cell death by membrane disruptions via their hydrophobicity, receptor-mediated pathways, activation of caspase pathway, or induction of NF-κB [68, 69]. Moreover, a recent study found that DCA treatment inhibited tumor progression by blocking cell proliferation through decreasing miR-92b-3p expression in an m6A-dependent posttranscriptional modification manner [70]. Therefore, several synthetic bile acid derivatives, such as HS-1183, HS-1199, HS-1200, LCA-TMA1 LCA-TMA3, have been designed and found useful to cancer therapy [71].

To date, the mechanism of the downregulation of bile acid metabolism in HCC remains largely unclear. It is also not clear if bile acid metabolism can be regulated by an RNA methylation-dependent mechanism. In our current study, we found that bile acid metabolic genes, such as BAAT, AKR1D1, SLC27A5 and CYP27A1, possessed RNA methylation sites. Furthermore, we revealed a complex crosstalk between m6A regulators and bile acid metabolism genes. We also observed a negative correlation between most RNA methylation regulators and bile acid metabolism regulators in HCC. These results indicated that the perturbation of RNA methylation was tightly associated with the downregulation of bile acid metabolism.

In conclusion, in the present study, we established and validated a classifier consisting of 7 RNA methylation regulators with independent prognostic value for HCC patients. Furthermore, we found that the primary bile acid biosynthesis pathway was downregulated in high-risk HCC patients, and the related metabolites (CDCA, CA, DCA, TDCA, and TCA) may be used as therapeutic targets for anti-HCC treatments. Moreover, our research revealed a potential crosstalk between bile acid and RNA methylation, uncovering a novel mechanism of the downregulation of bile acid metabolism in HCC and advanced our understanding on the oncogenic effect of RNA methylation regulators that contribute to the poor prognosis of HCC and are associated with the suppression of bile acid metabolism.

Acknowledgements

This work was supported by the National Natural Science Foundation of China (NO. 82070647 to Jiliang Wang, and 82071251 to Xiangdong Chen) and the National Key Research and Development Project (No. 2018-YFC2001802 to Xiangdong Chen).

Disclosure of conflict of interest

None.

Abbreviations

ACACA1, acetyl-CoA carboxylase 1; ACOX2, acyl-CoA oxidase 2; AKR1C4, aldo-keto reductase family 1, member C4; AKR1D1, aldo-keto reductase family 1, member D1; ALKBH1, alkB homolog 1, alpha-ketoglutaratedependent dioxygenase; ALKBH3, alkB homolog 3, alpha-ketoglutaratedependent dioxygenase; ALKBH5, alkB homolog 5, RNA demethylase; ALYREF, Aly/REF export factor; AMACR, alpha-methylacyl-CoA racemase; ATF4, activating transcription factor 4; AUC, area under the curve; BAAT, bile acid-CoA, amino acid N-acyltransferase; C/EBP-β, CCAAT enhancer binding protein-β; CA, cholic acid; CBLL1, Cbl proto-oncogene like 1; CCNA2, cyclin A2; CDCA, chenodeoxycholic acid; CDK2, cyclin-dependent kinase 2; CH-25H, cholesterol 25-hydroxylase; cMap, Connectivity Map; CPTAC, Clinical Proteomic Tumor Analysis Consortium; CREB1, CAMP responsive element binding protein 1; CSF1, colony stimulating factor 1; CYP27A1, cytochrome P450 family 27 subfamily A member 1; CYP39A1, cytochrome P450 family 39 subfamily A member 1; CYP46A1, cytochrome P450 family 46 subfamily A member 1; CYP7A1, cytochrome P450 family 7 subfamily A member 1; CYP7B1, cytochrome P450 family 7 subfamily B member 1; CYP8B1, cytochrome P450 family 8 subfamily B member 1; DCA, deoxycholic acid; DNMT1, DNA (cytosine-5-)-methyltransferase 1; DNMT3A, DNA methyltransferase 3 alpha; DNMT3B, DNA methyltransferase 3 beta; ELAVL1, ELAV like RNA binding protein 1; FMR1, fragile X mental retardation 1; FOXO1, Forkhead Box O1; FTO, fat mass and obesity associated; G6PC, glucose-6-phosphatase; GCA, glycocholic acid; GCDCA, glycochenodeoxycholic acid; GDCA, glycodeoxycholic acid; GSEA, gene set enrichment analysis; GSVA, gene set variation analysis; HCC, hepatocellular carcinoma; HDGF, hepatoma-derived growth factor; HNRNPA2B1, heterogeneous nuclear ribonucleoprotein A2/B1; HNRNPC, heterogeneous nuclear ribonucleoprotein C (C1/C2); HSD17B4, hydroxysteroid 17-beta dehydrogenase 4; ICGC, International Cancer Genome Consortium; IGF2BP1, insulin like growth factor 2 mRNA binding protein 1; IGF2BP2, insulin like growth factor 2 mRNA binding protein 2; IGF2BP3, insulin like growth factor 2 mRNA binding protein 3; KEGG, Kyoto Encyclopedia of Genes and Genomes; LASSO, Least Absolute Shrinkage and Selection Operation; LRPPRC, leucine rich pentatricopeptide repeat containing; m1A, N1-methyladenosine; m5C, 5-methylcytosine; m6A, N6-methyladenosine; METTL14, methyltransferase like 14; METTL3, methyltransferase like 3; NOP2, NOP2 nucleolar protein; NSUN2, NOP2/Sun RNA methyltransferase family member 2; NSUN3, NOP2/Sun RNA methyltransferase family member 3; NSUN4, NOP2/Sun RNA methyltransferase family member 4; NSUN5, NOP2/Sun RNA methyltransferase family member 5; NSUN6, NOP2/Sun RNA methyltransferase family member 6; NSUN7, NOP2/Sun RNA methyltransferase family member 7; PKM2, pyruvate kinase M2; RBM15, RNA binding motif protein 15; RBM15B, RNA binding motif protein 15B; ROC, receiver operating characteristic; SCD1, stearoyl-CoA desaturase 1; SCOS2, Suppressor of cytokine signaling 2; SCP2, sterol carrier protein 2; SLC27A5, solute carrier family 27 member 5; SOCS2, suppressor of cytokine signaling 2; SREBP1c, sterol regulatory element-binding protein 1c; STAT3, signal transducer and activator of transcription 3; TCA, taurocholic acid; TCDCA, taurochenodeoxycholic acid; TCGA, The Cancer Genome Atlas; TDCA, taurodeoxycholic acid; TET1, tet methylcytosine dioxygenase 1; TET2, tet methylcytosine dioxygenase 2; TET3, tet methylcytosine dioxygenase 3; TRMT10C, tRNA methyltransferase 10C, mitochondrial RNase P subunit; TRMT6, tRNA methyltransferase 6; TRMT61A, tRNA methyltransferase 61A; TRMT61B, tRNA methyltransferase 61B; USP3, ubiquitin-specific protease 3; WTAP, Wilms tumor 1 associated protein; YBX1, Y-box binding protein 1; YTHDC1, YTH domain containing 1; YTHDC2, YTH domain containing 2; YTHDF1, YTH N6-methyladenosine RNA binding protein 1; YTHDF2, YTH N6-methyladenosine RNA binding protein 2; YTHDF3, YTH N6-methyladenosine RNA binding protein 3; ZC3H13, zinc finger CCCH-type containing 13.

Address correspondence to: Yingli Nie, Department of Dermatology, Wuhan Children's Hospital (Wuhan Maternal and Child Healthcare Hospital), Tongji Medical College, Huazhong University of Science and Technology, Wuhan 430014, China. E-mail: yingli_nie@163.com; Xiangdong Chen, Department of Anesthesiology, Union Hospital, Tongji Medical College, Huazhong University of Science and Technology, Wuhan 430022, China. E-mail: xiangdongchen2013@163.com; Jiliang Wang, Department of Gastrointestinal Surgery, Union Hospital, Tongji Medical College, Huazhong University of Science and Technology, Wuhan 430022, China. E-mail: jiliang_wang@hust.edu.cn

References

[1] Siegel RL, Miller KD and Jemal A. Cancer statistics, 2019. CA Cancer J Clin 2019; 69: 7-34.

[2] Jonkhout N, Tran J, Smith MA, Schonrock N, Mattick JS and Novoa EM. The RNA modification landscape in human disease. RNA 2017; 23: 1754-1769.

[3] Michalak EM, Burr ML, Bannister AJ and Dawson MA. The roles of DNA, RNA and histone methylation in ageing and cancer. Nat Rev Mol Cell Biol 2019; 20: 573-589.

[4] Han X, Wang MK, Zhao YL, Yang Y and Yang YG. RNA methylations in human cancers. Semin Cancer Biol 2021; 75: 97-115.

[5] Esteve-Puig R, Bueno-Costa A and Esteller M. Writers, readers and erasers of RNA modifications in cancer. Cancer Lett 2020; 474: 127-137.

[6] Lan Q, Liu PY, Haase J, Bell JL, Hüttelmaier S and Liu T. The critical role of RNA m(6)A methylation in cancer. Cancer Res 2019; 79: 1285-1292.

[7] Chen MN and Wong CM. The emerging roles of N6-methyladenosine (m6A) deregulation in liver carcinogenesis. Mol Cancer 2020; 19: 44.

[8] Chen MN, Wei L, Law CT, Tsang FH, Shen JL, Cheng CL, Tsang LH, Ho DW, Chiu DK, Lee JM, Wong CC, Ng IO and Wong CM. RNA N6-methyladenosine methyltransferase-like 3 promotes liver cancer progression through YTHDF2-dependent posttranscriptional silencing of SOCS2. Hepatology 2018; 67: 2254-2270.

[9] Lin XY, Chai GS, Wu YM, Li JX, Chen F, Liu JZ, Luo GZ, Tauler J, Du J, Lin SB, He C and Wang HS. RNA m(6)A methylation regulates the epithelial mesenchymal transition of cancer cells and translation of Snail. Nat Commun 2019; 10: 2065.

[10] Li J, Zhu LJ, Shi YH, Liu JN, Lin L and Chen X. m6A demethylase FTO promotes hepatocellular carcinoma tumorigenesis via mediating PKM2 demethylation. Am J Transl Res 2019; 11: 6084-6092.

[11] Huang HL, Weng HY, Sun WJ, Qin X, Shi HL, Wu HZ, Zhao BS, Mesquita A, Liu C, Yuan CL, Hu YC, Hüttelmaier S, Skibbe JR, Su R, Deng XL, Dong L, Sun M, Li CY, Nachtergaele S, Wang YG, Hu C, Ferchen K, Greis KD, Jiang X, Wei MJ, Qu LJ, Guan JL, He C, Yang JH and Chen JJ. Recognition of RNA N(6)-methyladenosine by IGF2BP proteins enhances mRNA stability and translation. Nat Cell Biol 2018; 20: 285-295.

[12] Hou JJ, Zhang H, Liu J, Zhao ZJ, Wang JY, Lu ZK, Hu B, Zhou JK, Zhao ZC, Feng MX, Zhang HY, Shen B, Huang XX, Sun BC, Smyth MJ, He C and Xia Q. YTHDF2 reduction fuels inflammation and vascular abnormalization in hepatocellular carcinoma. Mol Cancer 2019; 18: 163.

[13] Ma JZ, Yang F, Zhou CC, Liu F, Yuan JH, Wang F, Wang TT, Xu QG, Zhou WP and Sun SH. METTL14 suppresses the metastatic potential of hepatocellular carcinoma by modulating N(6)-methyladenosine-dependent primary MicroRNA processing. Hepatology 2017; 65: 529-543.

[14] Zhang C and Jia GF. Reversible RNA Modification N(1)-methyladenosine (m(1)A) in mRNA and tRNA. Genomics Proteomics Bioinformatics 2018; 16: 155-161.

[15] Safra M, Sas-Chen A, Nir R, Winkler R, Nachshon A, Bar-Yaacov D, Erlacher M, Rossmanith W, Stern-Ginossar N and Schwartz S. The m1A landscape on cytosolic and mitochondrial mRNA at single-base resolution. Nature 2017; 551: 251-255.

[16] Dai XX, Wang TL, Gonzalez G and Wang YS. Identification of YTH domain-containing proteins as the readers for N1-methyladenosine in RNA. Anal Chem 2018; 90: 6380-6384.

[17] Woo HH and Chambers SK. Human ALKBH3-induced m(1)A demethylation increases the CSF-1 mRNA stability in breast and ovarian cancer cells. Biochim Biophys Acta Gene Regul Mech 2019; 1862: 35-46.

[18] Shimada K, Fujii T, Tsujikawa K, Anai S, Fujimoto K and Konishi N. ALKBH3 contributes to survival and angiogenesis of human urothelial carcinoma cells through NADPH oxidase and tweak/Fn14/VEGF signals. Clin Cancer Res 2012; 18: 5247-5255.

[19] Shi QM, Xue C, Yuan X, He YT and Yu ZJ. Gene signatures and prognostic values of m1A-related regulatory genes in hepatocellular carcinoma. Sci Rep 2020; 10: 15083.

[20] Bohnsack KE, Höbartner C and Bohnsack MT. Eukaryotic 5-methylcytosine (m5C) RNA methyltransferases: mechanisms, cellular functions, and links to disease. Genes (Basel) 2019; 10: 102.

[21] Nombela P, Miguel-López B and Blanco S. The role of m(6)A, m(5)C and Ψ RNA modifications in cancer: novel therapeutic opportunities. Mol Cancer 2021; 20: 18.

[22] Chellamuthu A and Gray SG. The RNA methyltransferase NSUN2 and its potential roles in cancer. Cells 2020; 9: 1758.
[23] Weissmann S, Alpermann T, Grossmann V, Kowarsch A, Nadarajah N, Eder C, Dicker F, Fasan A, Haferlach C, Haferlach T, Kern W, Schnittger S and Kohlmann A. Landscape of TET2 mutations in acute myeloid leukemia. Leukemia 2012; 26: 934-942.
[24] Li W and Xu LP. Epigenetic function of TET family, 5-methylcytosine, and 5-hydroxymethylcytosine in hematologic malignancies. Oncol Res Treat 2019; 42: 309-318.
[25] Takai H, Masuda K, Sato T, Sakaguchi Y, Suzuki T, Suzuki T, Koyama-Nasu R, Nasu-Nishimura Y, Katou Y, Ogawa H, Morishita Y, Kozuka-Hata H, Oyama M, Todo T, Ino Y, Mukasa A, Saito N, Toyoshima C, Shirahige K and Akiyama T. 5-hydroxymethylcytosine plays a critical role in glioblastomagenesis by recruiting the CHTOP-methylosome complex. Cell Rep 2014; 9: 48-60.
[26] Chen X, Li A, Sun BF, Yang Y, Han YN, Yuan X, Chen RX, Wei WS, Liu YC, Gao CC, Chen YS, Zhang MM, Ma XD, Liu ZW, Luo JH, Lyu C, Wang HL, Ma JB, Zhao YL, Zhou FJ, Huang Y, Xie D and Yang YG. 5-methylcytosine promotes pathogenesis of bladder cancer through stabilizing mRNAs. Nat Cell Biol 2019; 21: 978-990.
[27] Tibshirani R. Regression shrinkage and selection via the lasso. J R Statist Soc B 1996; 58: 267-288.
[28] Yu GC, Wang LG, Han YY and He QY. clusterProfiler: an R package for comparing biological themes among gene clusters. OMICS 2012; 16: 284-287.
[29] Wilkerson MD and Hayes DN. ConsensusClusterPlus: a class discovery tool with confidence assessments and item tracking. Bioinformatics 2010; 26: 1572-1573.
[30] Xuan JJ, Sun WJ, Lin PH, Zhou KR, Liu S, Zheng LL, Qu LH and Yang JH. RMBase v2.0: deciphering the map of RNA modifications from epitranscriptome sequencing data. Nucleic Acids Res 2018; 46: D327-D334.
[31] Deng S, Zhang HW, Zhu KY, Li XY, Ye Y, Li R, Liu XF, Lin DX, Zuo ZX and Zheng J. M6A2Target: a comprehensive database for targets of m6A writers, erasers and readers. Brief Bioinform 2021; 22: bbaa055.
[32] Deng FW, Chen D, Wei XL, Lu SL, Luo X, He JC, Liu JT, Meng TB, Yang AL and Chen HW. Development and validation of a prognostic classifier based on HIF-1 signaling for hepatocellular carcinoma. Aging (Albany NY) 2020; 12: 3431-3450.
[33] Huang YB, Chen S, Qin W, Wang YL, Li L, Li QX and Yuan XL. A novel RNA binding protein-related prognostic signature for hepatocellular carcinoma. Front Oncol 2020; 10: 580513.
[34] Tang CZ, Ma JK, Liu XL and Liu ZC. Identification of a prognostic signature of nine metabolism-related genes for hepatocellular carcinoma. PeerJ 2020; 8: e9774.
[35] Wang Z, Zhu J, Liu YJ, Liu CH, Wang WQ, Chen FZ and Ma LX. Development and validation of a novel immune-related prognostic model in hepatocellular carcinoma. J Transl Med 2020; 18: 67.
[36] Liang JY, Wang DS, Lin HC, Chen XX, Yang H, Zheng Y and Li YH. A novel ferroptosis-related gene signature for overall survival prediction in patients with hepatocellular carcinoma. Int J Biol Sci 2020; 16: 2430-2441.
[37] Liu GM, Zeng HD, Zhang CY and Xu JW. Identification of a six-gene signature predicting overall survival for hepatocellular carcinoma. Cancer Cell Int 2019; 19: 138.
[38] Wu XM, Zhang XJ, Tao LL, Dai XC and Chen P. Prognostic value of an m6A RNA methylation regulator-based signature in patients with hepatocellular carcinoma. Biomed Res Int 2020; 2020: 2053902.
[39] Zhang T, Nie YL, Gu J, Cai KL, Chen XD, Li HL and Wang JL. Identification of mitochondrial-related prognostic biomarkers associated with primary bile acid biosynthesis and tumor microenvironment of hepatocellular carcinoma. Front Oncol 2021; 11: 587479.
[40] Li RK, Wang YH, Zhang XX, Feng MX, Ma J, Li J, Yang XM, Fang F, Xia Q, Zhang ZG, Shang MY and Jiang SH. Exosome-mediated secretion of LOXL4 promotes hepatocellular carcinoma cell invasion and metastasis. Mol Cancer 2019; 18: 18.
[41] Ruan J, Zheng HY, Rong XD, Rong XM, Zhang JY, Fang WJ, Zhao P and Luo RC. Over-expression of cathepsin B in hepatocellular carcinomas predicts poor prognosis of HCC patients. Mol Cancer 2016; 15: 17.
[42] Yang X, Yang Y, Sun BF, Chen YS, Xu JW, Lai WY, Li A, Wang X, Bhattarai DP, Xiao W, Sun HY, Zhu Q, Ma HL, Adhikari S, Sun M, Hao YJ, Zhang B, Huang CM, Huang N, Jiang GB, Zhao YL, Wang HL, Sun YP and Yang YG. 5-methylcytosine promotes mRNA export - NSUN2 as the methyltransferase and ALYREF as an m(5)C reader. Cell Res 2017; 27: 606-625.
[43] Fan J, Wang K, Du X, Wang JS, Chen SL, Wang YM, Shi M, Zhang L, Wu XD, Zheng DH, Wang CS, Wang LT, Tian B, Li GH, Zhou Y and Cheng H. ALYREF links 3'-end processing to nuclear export of non-polyadenylated mRNAs. EMBO J 2019; 38: e99910.
[44] Wang JJ, Li YC, Xu BB, Dong J, Zhao HY, Zhao DX and Wu Y. ALYREF drives cancer cell proliferation through an ALYREF-MYC positive feedback loop in glioblastoma. Onco Targets Ther 2021; 14: 145-155.

[45] Wang JZ, Zhu W, Han J, Yang X, Zhou R, Lu HC, Yu H, Yuan WB, Li PC, Tao J, Lu Q, Wei JF and Yang HW. The role of the HIF-1α/ALYREF/PKM2 axis in glycolysis and tumorigenesis of bladder cancer. Cancer Commun (Lond) 2021; 41: 560-575.

[46] Nagy Z, Seneviratne JA, Kanikevich M, Chang W, Mayoh C, Venkat P, Du Y, Jiang C, Salib A, Koach J, Carter DR, Mittra R, Liu T, Parker MW, Cheung BB and Marshall GM. An ALYREF-MYCN coactivator complex drives neuroblastoma tumorigenesis through effects on USP3 and MYCN stability. Nat Commun 2021; 12: 1881.

[47] Xue C, Zhao YL, Li GL and Li LJ. Multi-omic analyses of the m(5)C regulator ALYREF reveal its essential roles in hepatocellular carcinoma. Front Oncol 2021; 11: 633415.

[48] Bell JL, Wächter K, Mühleck B, Pazaitis N, Köhn M, Lederer M and Hüttelmaier S. Insulin-like growth factor 2 mRNA-binding proteins (IGF2BPs): post-transcriptional drivers of cancer progression? Cell Mol Life Sci 2013; 70: 2657-2675.

[49] Gutschner T, Hämmerle M, Pazaitis N, Bley N, Fiskin E, Uckelmann H, Heim A, Groß M, Hofmann N, Geffers R, Skawran B, Longerich T, Breuhahn K, Schirmacher P, Mühleck B, Hüttelmaier S and Diederichs S. Insulin-like growth factor 2 mRNA-binding protein 1 (IGF2BP1) is an important protumorigenic factor in hepatocellular carcinoma. Hepatology 2014; 59: 1900-1911.

[50] Fan ZY, Gao Y, Zhang W, Yang GW, Liu PP, Xu LG, Wang JH, Yan ZP, Han H, Liu R and Shu MF. METTL3/IGF2BP1/CD47 contributes to the sublethal heat treatment induced mesenchymal transition in HCC. Biochem Biophys Res Commun 2021; 546: 169-177.

[51] Yang YC, Wu J, Liu FQ, He J, Wu F, Chen J and Jiang Z. IGF2BP1 promotes the liver cancer stem cell phenotype by regulating MGAT5 mRNA stability via m6A RNA methylation. Stem Cells Dev 2021; 30: 1115-1125.

[52] Pu J, Wang JC, Qin ZB, Wang AM, Zhang Y, Wu XJ, Wu Y, Li WC, Xu ZM, Lu Y, Tang QL and Wei HM. IGF2BP2 promotes liver cancer growth through an m6A-FEN1-dependent mechanism. Front Oncol 2020; 10: 578816.

[53] Wang JY and Lu AQ. The biological function of m6A reader YTHDF2 and its role in human disease. Cancer Cell Int 2021; 21: 109.

[54] Zhang CZ, Huang SZ, Zhuang HK, Ruan SY, Zhou ZX, Huang KJ, Ji F, Ma ZY, Hou BH and He XS. YTHDF2 promotes the liver cancer stem cell phenotype and cancer metastasis by regulating OCT4 expression via m6A RNA methylation. Oncogene 2020; 39: 4507-4518.

[55] Janin M, Ortiz-Barahona V, de Moura MC, Martínez-Cardús A, Llinàs-Arias P, Soler M, Nachmani D, Pelletier J, Schumann U, Calleja-Cervantes ME, Moran S, Guil S, Bueno-Costa A, Piñeyro D, Perez-Salvia M, Rosselló-Tortella M, Piqué L, Bech-Serra JJ, De La Torre C, Vidal A, Martínez-Iniesta M, Martín-Tejera JF, Villanueva A, Arias A, Cuartas I, Aransay AM, La Madrid AM, Carcaboso AM, Santa-Maria V, Mora J, Fernandez AF, Fraga MF, Aldecoa I, Pedrosa L, Graus F, Vidal N, Martínez-Soler F, Tortosa A, Carrato C, Balañá C, Boudreau MW, Hergenrother PJ, Kötter P, Entian KD, Hench J, Frank S, Mansouri S, Zadeh G, Dans PD, Orozco M, Thomas G, Blanco S, Seoane J, Preiss T, Pandolfi PP and Esteller M. Epigenetic loss of RNA-methyltransferase NSUN5 in glioma targets ribosomes to drive a stress adaptive translational program. Acta Neuropathol 2019; 138: 1053-1074.

[56] Jiang Z, Li S, Han MJ, Hu GM and Cheng P. High expression of NSUN5 promotes cell proliferation via cell cycle regulation in colorectal cancer. Am J Transl Res 2020; 12: 3858-3870.

[57] Macari F, El-Houfi Y, Boldina G, Xu H, Khoury-Hanna S, Ollier J, Yazdani L, Zheng G, Bièche I, Legrand N, Paulet D, Durrieu S, Byström A, Delbecq S, Lapeyre B, Bauchet L, Pannequin J, Hollande F, Pan T, Teichmann M, Vagner S, David A, Choquet A and Joubert D. TRM6/61 connects PKCα with translational control through tRNAi(Met) stabilization: impact on tumorigenesis. Oncogene 2016; 35: 1785-1796.

[58] Wang QY, Zhang QY, Huang YJ and Zhang JW. m(1)A regulator TRMT10C predicts poorer survival and contributes to malignant behavior in gynecological cancers. DNA Cell Biol 2020; 39: 1767-1778.

[59] Li YH, Zhang QY, Cui GS, Zhao F, Tian X, Sun BF, Yang Y and Li W. m(6)A regulates liver metabolic disorders and hepatogenous diabetes. Genomics Proteomics Bioinformatics 2020; 18: 371-383.

[60] Zhou B, Liu CZ, Xu LY, Yuan YW, Zhao JJ, Zhao WJ, Chen YY, Qiu J, Meng MY, Zheng Y, Wang DD, Gao X, Li XY, Zhao QH, Wei XH, Wu DJ, Zhang HJ, Hu C, Zhuo XZ, Zheng MH, Wang H, Lu Y and Ma XR. N(6)-methyladenosine reader protein YT521-B homology domain-containing 2 suppresses liver steatosis by regulation of mRNA stability of lipogenic genes. Hepatology 2021; 73: 91-103.

[61] Wu JM, Frazier K, Zhang JF, Gan ZD, Wang T and Zhong X. Emerging role of m(6) A RNA methylation in nutritional physiology and metabolism. Obes Rev 2020; 21: e12942.

[62] Wu RF, Liu YH, Yao YX, Zhao YL, Bi Z, Jiang Q, Liu Q, Cai M, Wang FQ, Wang YZ and Wang XX. FTO regulates adipogenesis by controlling cell

cycle progression via m(6)A-YTHDF2 dependent mechanism. Biochim Biophys Acta Mol Cell Biol Lipids 2018; 1863: 1323-1330.
[63] Zuo XL, Chen ZQ, Gao W, Zhang Y, Wang JG, Wang JF, Cao M, Cai J, Wu JD and Wang XH. M6A-mediated upregulation of LINC00958 increases lipogenesis and acts as a nanotherapeutic target in hepatocellular carcinoma. J Hematol Oncol 2020; 13: 5.
[64] Lin Y, Wei XL, Jian ZX and Zhang XW. METTL3 expression is associated with glycolysis metabolism and sensitivity to glycolytic stress in hepatocellular carcinoma. Cancer Med 2020; 9: 2859-2867.
[65] Yang NM, Wang T, Li QJ, Han F, Wang ZZ, Zhu RL and Zhou JX. HBXIP drives metabolic reprogramming in hepatocellular carcinoma cells via METTL3-mediated m6A modification of HIF-1α. J Cell Physiol 2021; 236: 3863-3880.
[66] Han J, Han ML, Xing H, Li ZL, Yuan DY, Wu H, Zhang H, Wang MD, Li C, Liang L, Song YY, Xu AJ, Wu MC, Shen F, Xie Y and Yang T. Tissue and serum metabolomic phenotyping for diagnosis and prognosis of hepatocellular carcinoma. Int J Cancer 2020; 146: 1741-1753.
[67] Fang YW, Han SI, Mitchell C, Gupta S, Studer E, Grant S, Hylemon PB and Dent P. Bile acids induce mitochondrial ROS, which promote activation of receptor tyrosine kinases and signaling pathways in rat hepatocytes. Hepatology 2004; 40: 961-971.
[68] Powell AA, LaRue JM, Batta AK and Martinez JD. Bile acid hydrophobicity is correlated with induction of apoptosis and/or growth arrest in HCT116 cells. Biochem J 2001; 356: 481-486.
[69] Payne CM, Weber C, Crowley-Skillicorn C, Dvorak K, Bernstein H, Bernstein C, Holubec H, Dvorakova B and Garewal H. Deoxycholate induces mitochondrial oxidative stress and activates NF-kappaB through multiple mechanisms in HCT-116 colon epithelial cells. Carcinogenesis 2007; 28: 215-222.
[70] Lin RR, Zhan M, Yang LH, Wang H, Shen H, Huang S, Huang XC, Xu SW, Zhang ZJ, Li WJ, Liu Q, Shi YS, Chen W, Yu JX and Wang J. Deoxycholic acid modulates the progression of gallbladder cancer through N(6)-methyladenosine-dependent microRNA maturation. Oncogene 2020; 39: 4983-5000.
[71] Kundu S, Kumar S and Bajaj A. Cross-talk between bile acids and gastrointestinal tract for progression and development of cancer and its therapeutic implications. IUBMB Life 2015; 67: 514-523.

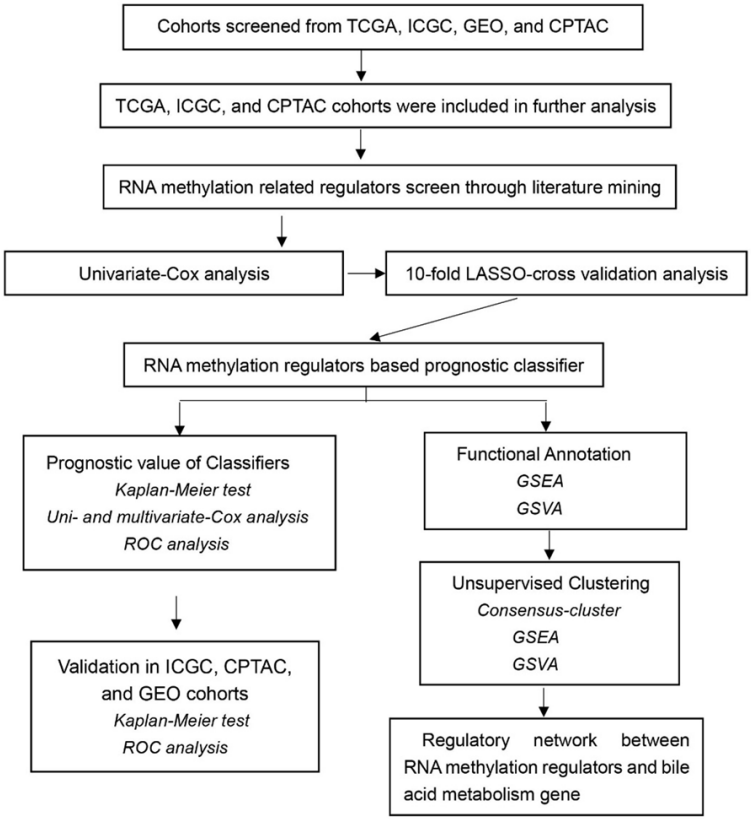

Figure S1. Flowchart of the construction of the RNA methylation regulators-based prognostic classifier. ROC: receiver operating characteristic; TCGA: The Cancer Genome Atlas; CPTAC: Clinical Proteomic Tumor Analysis Consortium; ICGC: International Cancer Genome Consortium; LASSO: The least absolute shrinkage and selection operation; GSVA: Gene set variation analysis; GSEA: Gene set enrichment analysis.

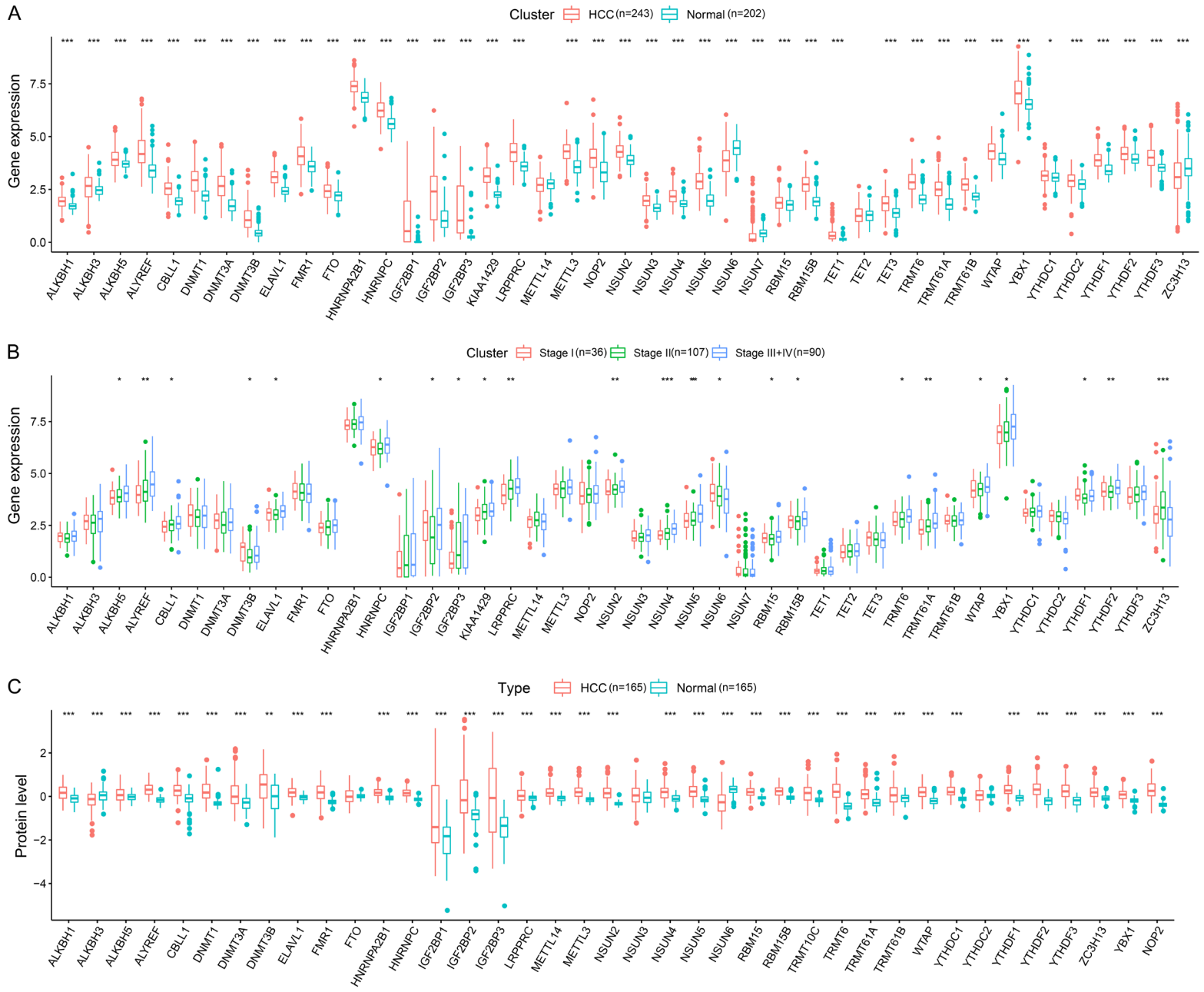
A
Cluster HCC (n=243) Normal (n=202)
Gene expression
B
Cluster Stage I (n=36) Stage II(n=107) Stage III+IV(n=90)
Gene expression
C
Type HCC (n=165) Normal (n=165)
Protein level

Figure S2. Expression landscape of RNA methylation regulators in HCC. A. Expression levels of RNA methylation regulators in HCC and adjacent normal tissues in the ICGC cohort by Student t test. B. Expression levels of RNA methylation regulators in different tumor stages of HCC in the ICGC cohort by Kruskal-Wallis test. C. Protein levels of RNA methylation regulators in HCC and adjacent normal tissues in the CPTAC cohort by Student t test.

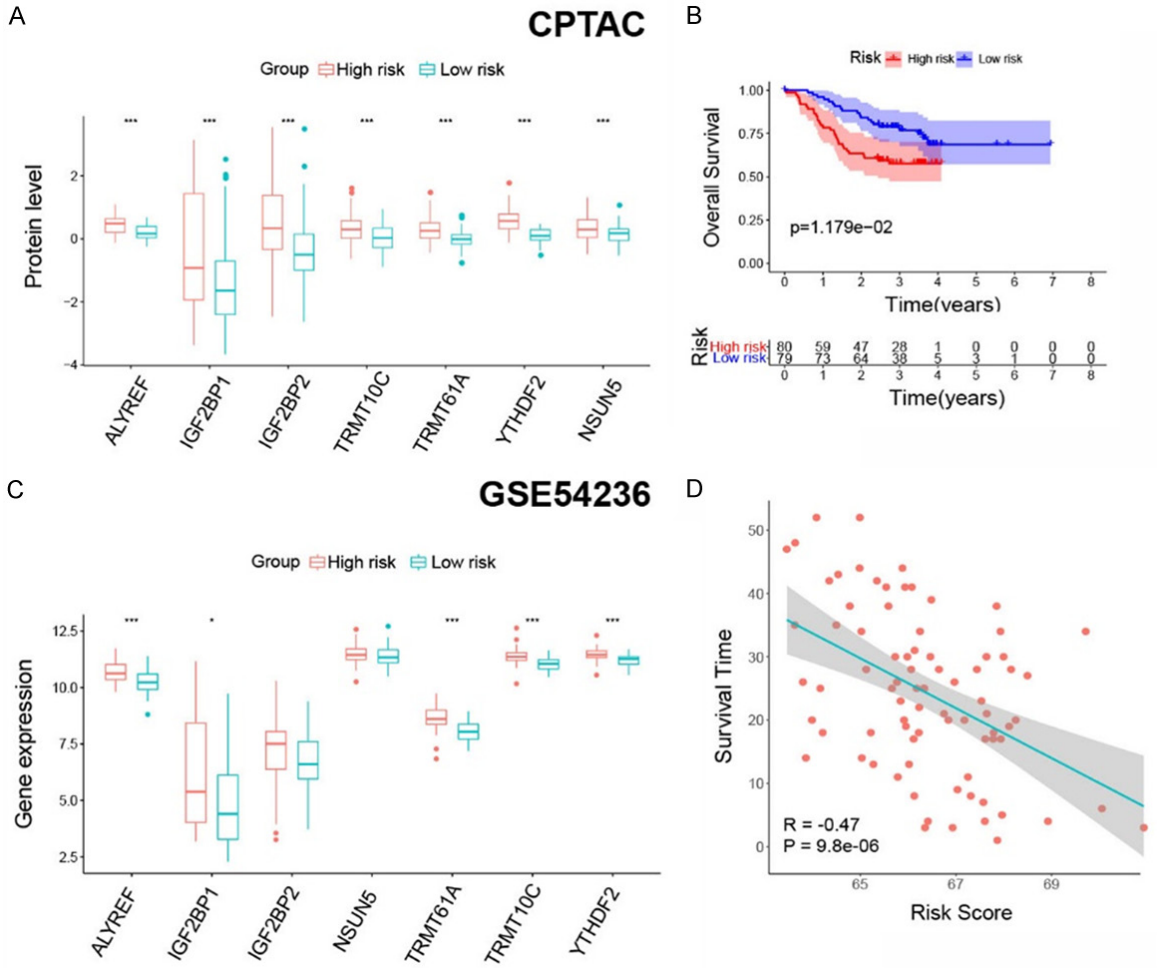

Figure S3. The prognostic value of the RNA methylation-based classifier in CPTAC cohort and GSE54236 cohort. A. Protein levels of all 7 regulators of the classifier in the high- and low-risk groups from the CPTAC cohort. *P<0.05; **P<0.01; ***P<0.001. B. Kaplan-Meier survival analysis of OS between the high- and low-risk patients from the CPTAC cohort. C. mRNA levels of all 7 regulators of the classifier in the high- and low-risk groups from the GSE54236 cohort. *P<0.05; **P<0.01; ***P<0.001. D. The relationship between survival time and risk score of HCC patients in the GSE54236 cohort.

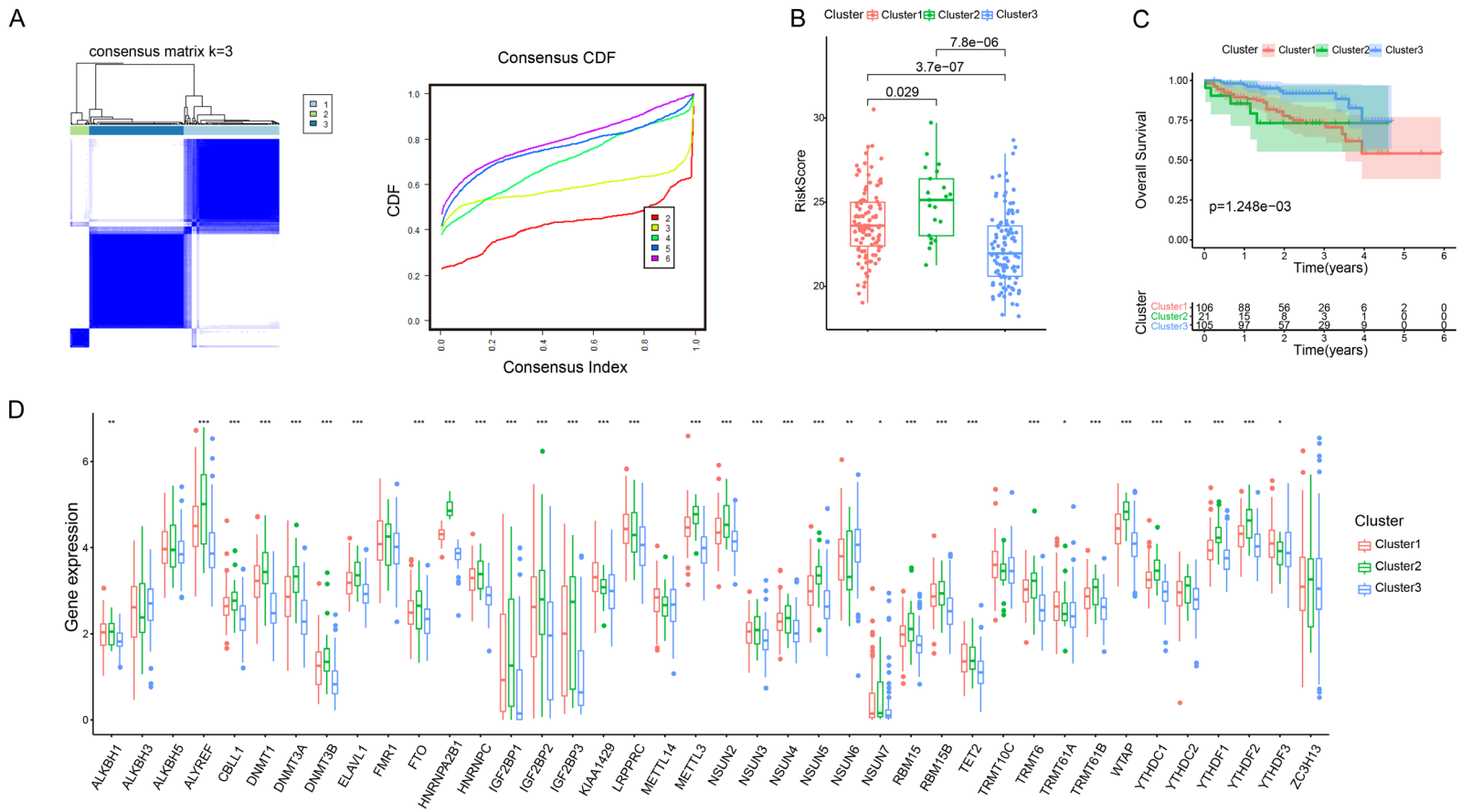
A
consensus matrix k=3
Consensus CDF
CDF
Consensus Index
B
Cluster Cluster1 Cluster2 Cluster3
7.8e−06
3.7e−07
0.029
RiskScore
C
Cluster Cluster1 Cluster2 Cluster3
Overall Survival
p=1.248e−03
Time(years)
Cluster1 106 88 56 26 6 2 0
Cluster2 21 15 8 3 1 0 0
Cluster3 105 97 57 29 9 0 0
D
Gene expression
Cluster
Cluster1
Cluster2
Cluster3
ALKBH1 ALKBH3 ALKBH5 ALYREF CBLL1 DNMT1 DNMT3A DNMT3B ELAVL1 FMR1 FTO HNRNPA2B1 HNRNPC IGF2BP1 IGF2BP2 IGF2BP3 KIAA1429 LRPPRC METTL14 METTL3 NSUN2 NSUN3 NSUN4 NSUN5 NSUN6 NSUN7 RBM15 RBM15B TET2 TRMT10C TRMT6 TRMT61A TRMT61B WTAP YTHDC1 YTHDC2 YTHDF1 YTHDF2 YTHDF3 ZC3H13

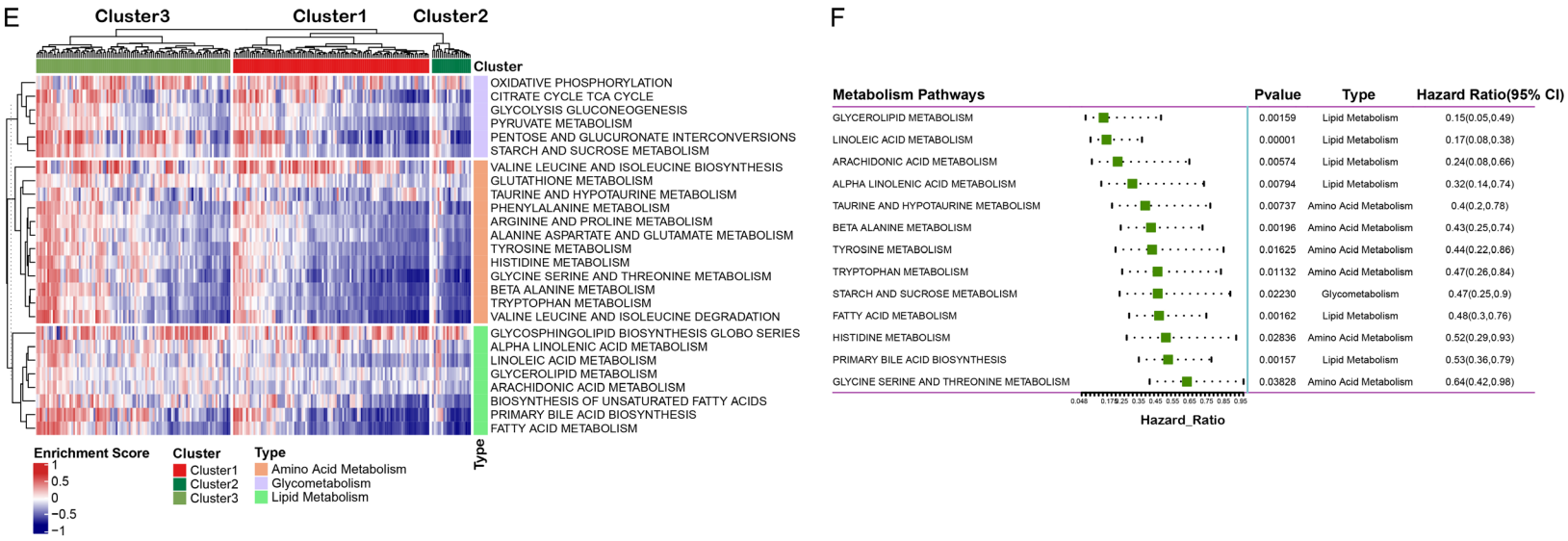

Figure S4. Unsupervised clustering based on RNA methylation regulators. A. Heatmaps of the consensus matrices for k=3. B. Differences of the risk score among 3 clusters in ICGC cohort by Wilcox test. C. Kaplan-Meier analysis of overall survival among 3 clusters in ICGC cohort. D. Differences in the expression of RNA methylation regulators among 3 clusters in ICGC cohort by Kruskal-Wallis test. E. GSVA analysis showed the activation states of metabolic pathways based on the KEGG database among 3 clusters in the ICGC cohort. F. Univariate Cox regression analysis of the activation of metabolic pathways with overall survival in the ICGC cohort.